



1 The benefits of increasing resolution in global and regional 2 climate simulations for European climate extremes

3 Carley E. Iles¹, Robert Vautard¹, Jane Strachan², Sylvie Jousaume¹, Bernd R. Eggen² and Chris
4 D. Hewitt²

5 ¹Laboratoire des Sciences du Climat et de l'Environnement, LSCE-IPSL, CEA-CNRS-UVSQ, Université
6 Paris-Saclay, F-91198 Gif-sur-Yvette, France

7 ²Hadley Centre, Met Office, Exeter, UK

8 *Correspondence to:* Carley E. Iles (carley.iles@lsce.ipsl.fr)

9 **Abstract.** Many climate extremes, including heatwaves and heavy precipitation events, are projected to worsen under
10 climate change, with important impacts for society. Future projections, required for adaptation, are often based on
11 climate model simulations. Given finite resources, trade-offs must be made concerning model resolution, ensemble
12 size and level of model complexity. Here we focus on the resolution component. A given resolution can be achieved
13 over a region using either global climate models (GCMs) or at lower cost using regional climate models (RCMs) that
14 dynamically downscale coarser GCMs. Both approaches to increasing resolution may better capture small-scale
15 processes and features (downscaling effect), but increased GCM resolution may also improve the representation of
16 large-scale atmospheric circulation (upscaling effect). The size of this upscaling effect is therefore important for
17 deciding modelling strategies. Here we evaluate the benefits of increased model resolution for both global and regional
18 climate models for simulating temperature, precipitation and wind extremes over Europe at resolutions that could
19 currently be realistically used for coordinated sets of climate projections at the pan-European scale. First we examine
20 the benefits of regional downscaling by comparing EURO-CORDEX simulations at 12.5 and 50 km resolution to their
21 coarser CMIP5 driving simulations. Secondly, we compare global scale HadGEM3-A simulations at three resolutions
22 (130, 60 and 25 km). Finally, we separate out resolution dependent differences for HadGEM3-A into downscaling and
23 upscaling components using a circulation analogue technique. Results suggest limited benefits of increased resolution
24 for heatwaves, except in reducing hot biases over mountainous regions. Precipitation extremes are sensitive to
25 resolution, particularly over complex orography, with larger totals and heavier tails of the distribution at higher
26 resolution, particularly in the CORDEX vs CMIP5 analysis. CMIP5 models underestimate precipitation extremes,
27 whilst CORDEX simulations overestimate compared to E-OBS, particularly at 12.5 km, but results are sensitive to the
28 observational dataset used, with the MESAN reanalysis giving higher totals and heavier tails than E-OBS. Wind
29 extremes are somewhat stronger and heavier tailed at higher resolution, except at coastal regions where large grid
30 boxes spread strong ocean winds further over land. The circulation analogue analysis suggests that differences with
31 resolution for the HadGEM3-A GCM are primarily due to downscaling effects.

32



33 **1 Introduction**

34 Climate extremes, such as heatwaves and heavy precipitation events are projected to worsen under climate change,
35 with important impacts for society (Seneviratne et al., 2012). Such projections are generally based on numerical climate
36 model simulations. However, given finite computational resources, trade-offs between model resolution, ensemble size
37 and the level of model complexity are necessary. For extreme events driven by large-scale processes such as long-
38 standing anticyclones, the proper simulation of the amplitude of extremes is limited by dynamics but also by land-
39 atmosphere feedbacks and the many physical processes involved in the surface energy budget. Such extremes are
40 typically heat waves, droughts and cold spells. Many other types of extreme event are by nature small scale. Such is
41 the case of convective precipitation, floods, extratropical wind storms, cyclones and medicanes. The resolution of
42 Global Climate Models (GCMs) in CMIP5 (Coupled Model Intercomparison Project Phase 5; Taylor et al., 2012) does
43 not allow these events to be resolved explicitly. Increased resolution in GCMs may improve the representation of
44 small-scale processes and features, including orography and coastlines (downscaling effect), but potentially may also
45 improve the representation of the interaction between small and large scale dynamical processes and ultimately
46 improve the large-scale atmospheric flow (upscaling effect). For instance, a better representation of baroclinic eddies
47 may help to better simulate large Rossby waves such as those inducing long-lived anomalies, due to the inverse energy
48 cascade. This may improve the simulation of the frequency and duration of heat waves and cold spells, and related
49 anomalies such as summer droughts. For precipitation and wind extremes, an improvement with resolution could be
50 expected due to the small-scale processes and features involved. However, upscaling effects may also have benefits
51 by improving storm-track location, and duration of wet spells. An alternative approach to increasing the resolution of
52 global-scale models is to use regional climate models (RCMs) driven by coarser GCMs to achieve a given high
53 resolution over a limited area at lower cost. However, this technique only captures downscaling effects, since the RCM
54 inherits the large scale circulation from the driving GCM.

55
56 Current generation GCMs commonly used for climate projections (e.g. CMIP5 models) have a resolution ranging from
57 about 70 to 250 km resolution, although 25 km GCMs are starting to be run under projects such as PRIMAVERA and
58 HighResMIP (part of CMIP6; Haarsma et al., 2016). For coordinated RCM experiments, such as CORDEX
59 (Coordinated Regional Downscaling Experiment; Giorgi et al., 2009), resolutions are generally between 10 to 50 km
60 (e.g. Jacob et al., 2014). In order to simulate convective precipitation a resolution of <5 km is really needed, which is
61 very computationally expensive, but such ensembles of convection permitting RCMs are currently in development
62 (Coppola et al., 2019). An important question is the extent to which increased resolution benefits the simulation of
63 extreme events for both global and regional models for the kind of resolutions that can realistically be run for
64 coordinated pan-continental climate projections. Particularly, whether using global high resolution adds further
65 benefits over regional high resolution due to an improved large scale circulation. We will address these questions
66 focusing on Europe, whose climate is highly variable and affected by a range of both large and small scale processes,
67 which present challenges for adequate simulation. We focus on extreme precipitation, temperature and wind, to cover
68 a range of events that may be affected by resolution in different ways.

69



70 The benefits of increased resolution for European precipitation extremes are well documented, whilst the effects on
71 heatwaves, cold spells and wind extremes are less well known. In GCMs, global precipitation tends to increase with
72 resolution, and for grid point models the fraction of land precipitation and moisture fluxes from land to ocean increases,
73 largely due to better resolved orography (Vannière et al., 2019; Terai et al., 2018; Demory et al., 2014). Precipitation
74 extremes tend to get heavier and agree better with observations (Wehner et al., 2010, O'Brien et al., 2016; Kopparla
75 et al., 2013; Shields et al., 2016; Vannière et al., 2019), unless the parameterisation schemes are not suited to the
76 resolution (e.g. Wehner et al., 2014). In Europe, Schiemann et al. (2018) find that both mean and extreme precipitation
77 are simulated better with increased resolution in HadGEM3A, mostly originating from better resolved orography. In
78 contrast, Van Haren et al. (2015a) find that improvements in Northern and Central European mean and extreme winter
79 precipitation with resolution are mostly associated with improved storm tracks in EC-Earth. For RCMs, extreme
80 precipitation is improved with resolution when compared to high resolution observations, particularly over orography,
81 including frequency-intensity distributions and spatial patterns, (see e.g. Torma et al., 2015 and Prein et al., 2016 for
82 EUROCORDEX at 12.5 km vs 50km and vs the driving GCMs, and Ruti et al., (2016) for Med-CORDEX). However,
83 benefits are smaller for regional and seasonal mean precipitation. Convection permitting models (<4km resolution) are
84 particularly beneficial in simulating summer extreme and sub-daily precipitation, including the diurnal cycle of
85 convection, but can overdo extreme precipitation (e.g. Prien et al., 2015; Kendon et al., 2012; 2014).

86

87 For heatwaves, increasing resolution does not lead to obvious benefits in RCM simulations (see e.g. Vautard et al.,
88 2013 for EURO-CORDEX), except improved spatial detail (Gutjahr et al., 2016). However, increased resolution may
89 have more impact in global models since the large scale circulation that contributes to their formation may be affected.
90 This remains a largely unstudied question, with the exception of a few studies such as Cattiaux et al. (2013) who find
91 that increasing resolution in the IPSL GCM leads to a reduction in the cold bias of both cold and warm extremes in
92 Europe, along with improved statistics, such as duration and frequencies and improved weather regimes.

93

94 For wind extremes, stronger winds and better spatial detail with resolution have been found for regional models (e.g.
95 Pryor et al., 2012; Kunz et al., 2010). Donat et al. (2010) found that observed storm loss estimates for Germany could
96 be reconstructed more accurately through dynamical downscaling compared to using the coarser resolution driving
97 ERA-40 data directly. Ruti et al., (2016) found improvements in Mediterranean cyclogenesis in coupled Med-
98 CORDEX RCMs relative to the ERA-interim driving data, whilst extreme winds over the Mediterranean generally
99 improve (i.e. are stronger) with higher resolution RCMs (e.g. Ruti et al. 2016; Hermann et al. 2011). However, most
100 GCM studies focus on the simulation of extratropical cyclones rather than wind directly. Such studies find an
101 improvement in the representation of various aspects of Northern Hemisphere extratropical cyclones with increased
102 resolution, including frequency, intensity and the position of the storm tracks (Colle et al., 2013; Jung et al., 2006;
103 2012), even in the higher resolution CMIP5 models (~<130 km; Zappa et al., 2013). Vries et al., (2019) found that the
104 resolution of Atlantic Gulf-Stream SST fronts affects winter extratropical cyclone strength. Whether these
105 improvements translate into an improvement in wind extremes remains to be assessed.

106



107 Persistence of weather regimes, such as blocking or the phase of the North Atlantic Oscillation, can be important
108 drivers for extreme events in Europe. Using the ECMWF IFS model, Dawson et al., (2012; 2015) find that such weather
109 regimes cannot be simulated realistically at typical CMIP5 resolution (~125 km), but are improved at 40 km, and well-
110 simulated at 16km. Cattiaux et al., (2013) find improvements at more modest resolutions in the IPSL model. Blocking
111 frequency tends to be underestimated by CMIP5-resolution climate models (Anstey et al., 2013). This tends to be
112 improved with resolution, particularly over the North Atlantic (Jung et al., 2012, Anstey et al., 2013; Matsueda et al.,
113 2009, Berckmans et al., 2013, Davini et al., 2017a; 2017b), although results tend to be somewhat sensitive to season
114 and model considered (Schiemann et al., 2017) and compensating errors may be involved (Davini et al., 2017a for EC-
115 EARTH). O'Reilly et al. (2016) find that having a well-resolved Gulf stream SST front is also important for European
116 winter blocking and associated cold spells. An important question is whether these improvements in the large scale
117 circulation translate into an improvement in the simulation of European climate extremes.

118

119 Here we examine the benefits of increased resolution for global models compared to regional models for the simulation
120 of European heatwaves, heavy precipitation events and wind storms. We further break down any resolution related
121 differences for a global model into upscaling and downscaling components. This will shed light on whether potential
122 improvements in the large scale circulation suggested in the literature translate into an improved representation of
123 climate extremes. This is an important consideration in choosing how to distribute finite resources between global and
124 regional models. We focus on the kind of models widely used to provide climate projections at a European scale,
125 applying a consistent approach across model types. Firstly, the benefits of regional dynamical downscaling are
126 explored by comparing EURO-CORDEX simulations at 50 and 12.5 km resolutions to their coarser driving CMIP5
127 GCMs. Secondly, the benefits of increased resolution for a global model are examined using HadGEM3-A at 130, 60
128 and 25 km resolution. Finally, the roles of upscaling versus downscaling will be examined using a circulation analogue
129 technique applied to HadGEM3-A.

130 **2 Observational and model data**

131 **2.1 Observations**

132 Model simulations are evaluated using observational datasets. For daily precipitation and daily maximum temperature,
133 we use the gridded station based dataset E-OBS on a 0.5° latitude-longitude grid (Haylock et al. 2008). This covers
134 the European domain from 1950 to present. Gridded datasets tend to reduce the magnitude of extremes compared to
135 station data through smoothing effects, but are more comparable to the grid box averages from GCMs (Haylock et al.
136 2008). Nevertheless, E-OBS has a relatively low underlying station density, and tends to underestimate precipitation
137 extremes relative to higher density regional datasets), due to missed extremes which are local in scale (Prein and Gobiet
138 2017). However, such high resolution datasets are not available at a pan-European scale. As a compromise, results are
139 repeated for precipitation extremes using the MESAN reanalysis (Landelius et al. 2016), which combines information
140 from the high resolution HIRLAM reanalysis (Dahlgren et al. 2016) with a network of station-based observations. For
141 much of Europe these are the same as those used for E-OBS, but with the addition of Swedish Meteorological and



142 Hydrological Institute (SMHI) stations over Sweden, and a high density of Meteo-France stations over France
143 (Landelius et al. 2016). MESAN provides daily precipitation data for the more limited period 1989-2010. We use the
144 version available on a 0.11° rotated grid. Prein and Gobiet (2017) find that it gives heavier extremes than E-OBS in
145 some regions (France, Spain, the Carpathians), but generally not as high as the high resolution regional datasets (except
146 in France). Neither dataset is corrected for gauge undercatch, which tends to be around 3-20% for rain, and up to 40%
147 for snow, or even 80% for non-shielded gauges (Førland and Instituttt 1996; Goodison et al. 1997).

148

149 Wind extremes tend to happen on sub-daily time scales, necessitating the use of sub-daily data to avoid missing as
150 many events (although events, or their peak magnitude, will still be missed). We use three observational wind datasets.
151 These are all based on the ERA-Interim reanalysis (Dee et al. 2011), but differ in the way they are processed. The first
152 is the WFDEI dataset (WATCH-Forcing-Data-ERA-Interim; Weedon et al. 2014) and the other two are ECEM datasets
153 (European Climate Energy Mixes; Jones et al. 2017). One ECEM dataset is bias corrected using a Weibull distribution
154 based on the HadISD station dataset (Dunn et al. 2012) applied to each grid cell (ECEM-wbc), whereas the other
155 version contains no bias correction (ECEM-noc). WFDEI is available at 3 hourly resolution, whereas ECEM is 6
156 hourly. Therefore, 6 hourly data is used from both datasets for consistency. All datasets are available on a 0.5° regular
157 latitude longitude grid for the period 1979-2016. Although neither ECEM-noc or WFDEI are bias corrected, they
158 nevertheless give different values, presumably due to differences in interpolation method from the original 0.7° grid
159 of ERA-Interim.

160 **2.2 Climate model data**

161 **2.2.1 EURO-CORDEX and CMIP5**

162 In order to examine the effect of dynamical downscaling for climate extremes, we make use of the EURO-CORDEX
163 (Jacob et al. 2014) RCM simulations for the historical period over the European domain which are driven by lower
164 resolution global scale coupled CMIP5 GCMs. The GCMs are forced by observed records of anthropogenic and natural
165 forcings, such as greenhouse gases, anthropogenic aerosols, land use changes, solar variability and volcanic aerosols
166 to allow comparability to historical records. For the most part the RCMs inherit the effects of these forcing agents from
167 the GCMs, with the exception of greenhouse gases, which are prescribed. A comparison of the RCM simulations with
168 their driving CMIP5 simulations allows us identify any value added by regional high resolution. The EURO-CORDEX
169 simulations are available at 0.11° and 0.44° (12.5 km and 50 km respectively), allowing an assessment of the difference
170 that increased regional resolution brings. By examining the subset of GCM-RCM combinations that are common to
171 both CORDEX resolutions along with their driving GCMs we can isolate the effects of changing resolution.

172

173 Daily precipitation (pr), daily maximum temperature (tasmax), and daily maximum surface wind speed (sfcWindmax)
174 were taken from both CORDEX and CMIP5. The simulations used are shown in Table S1. This consists of 23 and 19
175 simulations for precipitation for the 0.44 and 0.11 simulations respectively, with 15 common to both categories with
176 data also available from their driving GCMs (from now on referred to as “common to all” or “common subset”); 22
177 and 18 respectively for temperature, with 14 common to all, and 15 and 14 for wind with 6 that are common to all. We



178 also extend the analysis to all other historical CMIP5 GCMs with the relevant variables, with 126 simulations from 41
179 GCMs for precipitation, 115 from 39 models for temperature and, 61 simulations from 28 models for wind. For wind,
180 using 3 or 6 hourly data would have made results more comparable to the observational wind datasets (see above).
181 However, such data were not available for the 0.44° CORDEX simulations, and for only three CORDEX simulations
182 at 0.11° resolution which also had data for their driving GCMs, all three of which use the same RCM (RCA). We
183 therefore use the variable sfcWindmax (daily maximum surface wind speed) which was available for many models.
184 The implications of this are discussed further in the results section.

185 **2.2.2 UPSCALE simulations**

186 In order to examine the benefits or otherwise of differences in resolution for a global model, we make use of simulations
187 undertaken as part of the UPSCALE project (UK on PRACE: weather-resolving Simulations of Climate for global
188 Environmental risk; Mizielinski et al. 2014). This consists of the atmosphere only version of the Hadley Centre Global
189 Environment Model 3 (HadGEM3-A) run at three different resolutions: N96 (130 km), N216 (60 km) and N512 (25
190 km), all with 85 vertical levels for the period 1985-2011, with 5, 3 and 5 ensemble members respectively (or 3, 3 and
191 5 for wind data). The simulations are forced by observed records of greenhouse gases, aerosols, ozone, solar variability
192 and volcanic forcings following the AMIP-II procedure (Taylor et al. 2000), and an alternative dataset for sea surface
193 temperatures (SSTs) and sea ice. Very few parameters differ between the resolutions, enhancing the comparability of
194 the three ensembles. We use daily precipitation data, daily maximum temperatures and 3-hourly wind (subsamped to
195 6-hourly).

196 **2.2.3 Regridding**

197 In order to compare models of different resolutions with each other and with observations it was necessary to regrid
198 variables to a common grid. We use a 0.5° regular longitude-latitude grid since it is the resolution of the majority of
199 the observational datasets used (E-OBS, ECEM and WFDEI) and is computationally feasible. Some of the benefits of
200 higher resolution may be lost by doing this, putting our results on the conservative side. However, sensitivity tests
201 showed that results for MESAN did not change perceptibly by using a 0.5° grid as compared to a 0.1° regular grid
202 (chosen to be close to the original 0.11° rotated grid). We regrid the daily data, before the calculation of annual extreme
203 indices.

204

205 Sensitivity of results to regridding technique was investigated for precipitation and wind for a number of models of
206 different resolutions and compared with results based on using the original grids (Figure S1). For the coarser resolution
207 models (e.g. HadCM3) results for precipitation extremes were very sensitive to regridding technique, with much
208 weaker extremes for some techniques e.g. distance-weighted average remapping and bilinear interpolation, with
209 unrealistic artefacts in the spatial patterns for many methods. For high resolution models, regridding technique did not
210 make much difference to results. Overall the nearest neighbour method was chosen since it gave results very close to
211 using the original grid for all model resolutions, preserving the amplitude of extremes, and also having minimal
212 artefacts when plotting spatial patterns of precipitation extremes. Whilst nearest neighbour may not be the best choice



213 in regridding from high resolution to lower (e.g. for MESAN and CORDEX 0.11), since information from only a
214 subset of grid cells is incorporated, results were the same when repeated using bicubic remapping. Results for wind
215 for the coarser models were also sensitive to regridding technique; the nearest neighbour method was again chosen
216 since it also performed well here, both in terms of minimising artefacts and replicating results using the original grid.
217 For temperature, which tends to be more uniform over large areas, bilinear interpolation was used, since the choice of
218 regridding technique is anticipated to be less important.

219 **3 Methods**

220 **3.1 Extremes Indices**

221 In order to examine extremes, we adopt indices based on the ETCCDI indices (Zhang et al. 2011). For precipitation
222 these are the annual maximum daily precipitation (Rx1day) and the annual maximum consecutive 5-day total
223 (Rx5day). For temperature we use the annual maximum daily maximum temperature (TXx) and the annual maximum
224 consecutive 5-day mean of daily maximum temperature (TXx5day). For wind we use the annual maximum of daily
225 maximum wind, which we refer to as (WindXx). This is based on sfcWindmax for the CMIP5 and CORDEX models,
226 and on 6-hourly data for the UPSCALE simulations and the observational wind datasets. These are therefore much
227 more rare extremes than those based e.g. on the 95th or even 99th percentile which would happen on average 1 in 20
228 days and 1 in 100 days respectively.

229
230 In order to examine how well the climate models simulate extremes and the differences between different resolutions,
231 we first examine the spatial patterns of the climatological mean values of the indices and their biases with respect to
232 observations. We then examine return period plots (see definitions below) for a number of regions for each index,
233 which highlights any differences in the shape of the tails of the distribution of the extremes. The regions used are based
234 on the PRUDENCE regions (Christenson and Christenson 2007) and the IPCC SREX regions (Seneviratne et al. 2012)
235 and are shown in Figure S2 and Table S2. A subset of representative regions are presented here, with some comments
236 about the others.

237 **3.2 Return periods**

238 In order to calculate regional return periods and return values we first sort the data into ascending order for each grid
239 cell, and then calculate the area weighted regional averages. The return periods are calculated as N/k where N is the
240 number of years of data, and k is the rank, with $k=1$ for the largest value. Return periods are therefore the inverse of
241 the probability of an event exceeding a given value (called the “return value”). The regional average is made, for given
242 return periods, over the associated return values. To avoid complications from missing data, grid cells in E-OBS with
243 more than 5 days of missing data in any year during the period examined were masked for the whole period. Having
244 one or more years missing would complicate the calculation of regional mean return periods and values. Models and
245 observational datasets are masked to have the same spatial coverage, which is land only. A common time period, across
246 the models being examined and the observations they are being compared to, are chosen to allow comparability. For



247 the CMIP5 and CORDEX analysis 1970-2005 is used for temperature and precipitation and 1979-2005 for wind. For
248 the UPSCALE runs we use 1985-2011 for temperature, and 1989-2010 for precipitation to allow comparisons with
249 MESAN (1986-2011 is used for the analogue analysis, see below) and 1986-2011 for wind.

250

251 Return values and periods are also calculated for the “pooled ensemble”. For each grid cell, all simulations of a certain
252 type are combined into one long time series before being sorted into ascending order, and then regional means are
253 calculated as above. The models are first bias adjusted by subtracting the difference between their climatology of the
254 index in question and the climatology of the observations at a grid cell level. This adjustment avoids, for example,
255 models with particularly hot extremes dominating the ends of the tails of the distributions and allows differences in
256 the shapes of the distribution tails of different models to be compared more easily. Figure S3 shows the resulting spread
257 of models across the distributions.

258

259 In order to allow comparability of results between the EURO-CORDEX ensembles at both resolutions and their driving
260 CMIP5 GCMs, we picked a subset of models that are consistent across each category; that is the same GCM-RCM
261 combinations are used across both the 0.11 and 0.44° CORDEX categories, and are compared to the CMIP5 model
262 runs that were used to drive them (Table S1). We refer to these simulations as the “common subset” (see section 2.2.1).
263 The only exception is that the EC-EARTH ensemble member “r3” was not available for download from ESGF, so r2
264 was substituted instead. Since more than one EURO-CORDEX RCM is driven by the same ensemble member of the
265 same GCM, we repeat these GCMs when calculating the CMIP5 ensemble mean and pooled results for the common
266 subset. For the UPSCALE simulations, since the same version of the same model is used across each resolution, results
267 can also be examined without bias adjusting the extremes climatology, and this provides some interesting insights.

268

269 Confidence intervals are calculated using a bootstrapping method. If, for example, the analysis period was 1970-2005
270 (i.e. 36 years), 1000 random samples of 36 years from this period are chosen from the same observations/ simulation(s),
271 allowing the same year to be chosen more than once per iteration. For each random sample, the chosen values are
272 sorted for each grid cell and a regional average is calculated as above, effectively yielding 1000 return period curves
273 per region. The 5th and 95th percentile of these values are then calculated to give the confidence intervals.

274

275 Finally, for the HadGEM3-A GCM simulations, a circulation analogue technique is used to split any differences in
276 results according to resolution into upscaling (i.e. improved large scale circulation) and downscaling effects. This is
277 described in section 4.3.



278 **4 Results**

279 **4.1 The benefits of regional high resolution: EURO-CORDEX versus CMIP5**

280 **4.1.1 Temperature extremes**

281 Figure 1 shows the spatial patterns of the climatological mean of TXx5day for the period 1970-2005 for E-OBS, and
282 the multi-model means (MMM) of CMIP5, and CORDEX at both resolutions, along with their biases with respect to
283 E-OBS. The first two columns are based on a subset of CORDEX simulations that use the same GCM-RCM
284 combinations at both resolutions, whilst the CMIP5 MMM is based only on the CMIP5 simulations that drive these
285 RCMs, with repetition of the GCMs that drive more than one RCM. The last two columns are based on the mean of
286 all available simulations for each category to check how representative the results based on the subset are of the whole
287 ensembles. The same general pattern can be seen in both the observations and the models, with hotter extremes in the
288 south and cooler extremes in the north and over the mountains. At higher resolution the colder extremes over the Alps
289 and Carpathians become more distinct. For the “common subset” the pattern of biases relative to E-OBS is similar for
290 each model category with cold biases in the North and West and hot biases in the South-East. However, the hot biases
291 over the mountains reduce with higher resolution since the model topography is higher. The cold bias over Scandinavia
292 is also larger in CORDEX than in CMIP5. Biases using the whole ensemble are very similar as those for the CORDEX
293 subset, although for CMIP5 the hot biases over the south-east, and over mountain ranges are stronger. Findings for
294 TXx are similar, but hotter (not shown).

295

296 To give an idea of the level of consistency of results between models, results for individual models are shown in figure
297 S4. Although the CMIP5 models agree on the general spatial pattern of temperature extremes, their absolute
298 magnitudes vary considerably, although all are too hot over the Alps. There are also substantial differences between
299 results from different RCMs, including those driven by the same GCM. Biases of individual RCMs do not appear
300 systematically smaller than that of their driving GCM. Patterns are very similar for the same GCM-RCM chains at the
301 both 12.5 and 50 km resolutions. Results for different ensemble members of the same GCM or GCM-RCM chain are
302 very consistent, suggesting that the differences between models are not due to internal variability.

303

304 In order to assess the shape of the statistical distribution of temperature extremes, figure 2 (left column) shows return
305 period against magnitude for TXx5day for CMIP5, CORDEX at both resolutions and E-OBS, for individual models
306 (thin lines) and the pooled ensembles (circles) both for the common subset of models (darker circles) and all models
307 (lighter circles) (see Methods). Results are shown for Northern, Central and Southern Europe, and are representative
308 of the subregions. There is no obvious difference in the shape of the tails between CMIP5 and CORDEX, apart from
309 marginally heavier tails for CORDEX 0.44 in central Europe. Agreement with E-OBS is good for the pooled ensemble,
310 although many individual ensemble members lie outside the range of the observational uncertainty, particularly on the
311 heavy tailed side.

312



313 In summary, temperature extremes appear to be relatively insensitive to dynamical downscaling based on comparing
314 CMIP5 to CORDEX at 0.11° and 0.44° , except over mountains where hot biases decrease with resolution.

315 4.1.2 Precipitation extremes

316 Now we consider precipitation extremes for CMIP5 compared to CORDEX. Figure 3 shows the climatological mean
317 of Rx1day over the period 1970–2005 for E-OBS and the MMMs of CMIP5 and CORDEX at both resolutions, and
318 their biases with respect to E-OBS. The left two columns show results for the “common subset” of simulations across
319 the model categories, and the right two columns for all simulations. The heaviest annual maximum precipitation totals
320 in E-OBS occur over the Alps and the western side of coastal mountain ranges, including western Norway and north-
321 eastern Spain. A similar spatial pattern of precipitation distribution can be seen in the models, although totals are lower
322 in CMIP5, and higher in CORDEX. CMIP5 exhibits a dry bias over most of Europe, particularly over the areas of
323 maximum precipitation in E-OBS (i.e. over or near mountains), whilst CORDEX exhibits a general wet bias,
324 particularly in these same locations, and at higher resolution. Results using the entire ensembles are very similar to
325 using the common subset of simulations. Previous studies suggest that E-OBS underestimates precipitation extremes
326 since it is not corrected for gauge undercatch and has a relatively low underlying station density (e.g. Prein and Gobiet
327 2017). Therefore, we also repeat results relative to the MESAN reanalysis (Figure S5) for the shorter period 1989-
328 2005. MESAN uses a particularly high density of stations in France (see Data section). The climatology of Rx1day is
329 wetter in MESAN than in E-OBS over most of Europe, most noticeably over the Alps and surrounding areas. This
330 leads to the dry bias in CMIP5 appearing bigger, and the wet bias in CORDEX decreasing, although it is still present
331 in the 0.11° simulations. Using regional-scale very high resolution datasets could improve agreement with the 0.11°
332 simulations, since they tend to give heavier precipitation extremes (Prein and Gobiet 2017). Gauge undercatch could
333 also contribute to the difference.

334

335 Figure S6 shows results for individual models. Again, whilst models agree on the general pattern of precipitation
336 extremes – i.e. wettest over mountains, there are considerable inter-model differences concerning the magnitude,
337 particularly over complex orography. A number of CMIP5 models have too light extremes everywhere, but all
338 underestimate precipitation extremes over mountainous regions to a greater or lesser extent. RCMs systematically
339 simulate heavier precipitation extremes compared to their driving GCMs, particularly over mountains, and these
340 extremes tend to become heavier when moving from 0.44° to 0.11° in most cases. Many of the RCMs show a heavy
341 bias over much of Europe at 0.44° , although this may disappear if compared to MESAN, and this bias gets bigger at
342 higher resolution and is largest over mountainous regions. Again results are very consistent between ensemble
343 members of the same models.

344

345 Figure 2 (middle column) shows return period curves for Rx1day for Northern, Central and Southern Europe. There is
346 a clear separation in the tails of the distribution according to resolution, with CMIP5 having the lightest tails, CORDEX
347 0.44 in the middle, and CORDEX 0.11 with the heaviest tails across all regions (including the subregions – not shown).
348 Results using the common subset of models or the full ensembles are similar to each other. In order to compare with



349 observations, E-OBS should be compared to the thin lines for individual models rather than the pooled ensemble
350 results, since pooling seems to affect the shape of the distribution, causing it to lie below that of the single models.
351 EOBS tends to lie at the heavy end of the CMIP5 range for southern Europe, between CMIP5 and CORDEX 0.44 for
352 central Europe, and closer to CORDEX 0.44 in northern Europe. Using MESAN gives slightly heavier tails in central
353 Europe (figure S7) (particularly in France, where station density is highest –not shown) and more so in southern
354 Europe, causing the best agreement to occur with CORDEX 0.44 everywhere. Results for Rx5day are similar, but with
355 marginally less separation between the resolutions, whilst over Northern and Central Europe the best agreement with
356 E-OBS happens at a slightly higher resolution than for Rx1day – i.e. either with CORDEX 0.44 or the lower end of
357 the range of CORDEX 0.11 (not shown).

358

359 In summary, precipitation extremes are wetter and heavier tailed with higher resolution, especially over mountainous
360 regions. CMIP5 has a dry bias, particularly over mountains, whilst CORDEX tends to be too wet, particularly at 0.11°,
361 but results are sensitive to observational dataset used, with wet biases for CORDEX reducing when compared to the
362 higher resolution MESAN dataset.

363 **4.1.3 Wind Extremes**

364 Finally, we examine annual maximum wind (WindXx). Figure 4 shows the multi model means of climatological mean
365 annual maximum wind over the period 1979-2005 for CMIP5 and CORDEX at 0.44° and 0.11° for the common subset
366 of simulations and for all simulations compared to three observational datasets. Note however that the model results
367 are based on the annual maximum of the daily maximum of surface wind (variable “sfcWindmax”), whilst the
368 observations are based on the annual maximum of 6-hourly data. For CMIP5 models that had both sfcWindmax and
369 3-hourly data, we compared results using sfcWindmax, 3-hourly and 6-hourly data (Figure S8). 6-hourly data tends to
370 give lower values than using 3-hourly data or sfcWindmax since some events will be missed due to the lower sampling
371 frequency. In addition, sfcWindmax does not always appear calculated the same way across all models- although it
372 often gives higher wind speeds than using 3-hourly or 6-hourly data, the degree to which this is the case seems to
373 depend on the model, and suggests a different sampling frequency, whilst for a few models sfcWindmax gives the
374 lowest wind speeds. Ideally an analysis based on a consistent metric across models, such as 3 hourly or 6 hourly wind
375 speeds, would be performed. However, CORDEX at 0.44° does not have this data available, whilst CORDEX at 0.11°
376 only has it for a small number of simulations, all of which are based on RCA, and only 3 of which have data for the
377 driving GCM. Therefore, the reader is invited to interpret results with this caveat in mind. Model sfcWindmax
378 estimates may also differ in terms of the treatment of surface roughness length and the method for calculating wind at
379 10m from wind at a higher level.

380

381 All three observational datasets are based on ERA-interim, but WFDEI and ECEM-noc are processed differently,
382 whilst ECEM-wbc is bias corrected using a Weibull distribution based on the station based dataset HadISD (see Data
383 section). It is notable that all three datasets give different results, particularly ECEM-wbc, despite all being based on
384 ERA-Interim. WFDEI and ECEM-noc show the same overall pattern of annual maximum wind, with a belt of stronger



385 winds running zonally across the middle of Europe, including particularly high wind speeds over the British Isles, with
386 lower wind speeds to the north and south of this band. ECEM-noc has slightly faster wind speeds everywhere. ECEM-
387 wbc is very different with very high maximum wind speeds over southern Europe and Scandinavia, which are areas
388 with low wind speeds in the other two datasets. These differences are most apparent for wind extremes- the
389 climatological means of 6-hourly wind speeds are shown in Figure S9. Although patchier in nature, mean wind in
390 ECEM-wbc appears broadly similar to the other datasets. However, whilst the other two datasets have similar spatial
391 patterns between mean and extreme wind, for ECEM-wbc the patterns are very different. One assumption is that the
392 Weibull correction works well for mean wind, but is not suited to extremes, which are more sensitive to the parameters
393 of the Weibull correction. It should also be noted that as a reanalysis, ERA-interim is itself model based, albeit with
394 assimilation of observations.

395

396 The CMIP5 driving model mean shows a similar overall pattern of WindXx as WFDEI and ECEM-noc, with a pattern
397 of weaker winds in the north and south, and a belt of stronger winds in the middle, but with a lower magnitude than
398 the observations. Using the whole CMIP5 ensemble gives slightly stronger extreme winds. Absolute magnitudes are
399 not directly comparable to the observational estimates, which would be expected to have slightly slower winds, but
400 they are nevertheless broadly similar to WFDEI and ECEM-noc, but with too light winds in the central zonal belt. The
401 CORDEX multi model means show generally higher wind speeds, and a different spatial pattern, with the highest wind
402 speeds along western coastlines and over mountainous terrain. Differences between the 0.11° and 0.44° runs appear
403 small. Results for the common subset of simulations are very similar to those obtained from the complete CORDEX
404 ensembles. Biases are not shown due to the difference in temporal resolution with respect to the observations.

405

406 Figure S10 shows that there is a large variety between different models, particularly for CMIP5, but also according to
407 RCM. CanESM2 and IPSL-CM5A-LR are notable outliers, and this may be related to the timestep of the wind data
408 used to calculate sfcWindmax in these models. The zonal tripole pattern can be seen in a number of GCMs, as can
409 stronger winds along western and Mediterranean coastlines, and lower wind speeds over the Alps. Spatial patterns for
410 the RCMs are very RCM specific and relatively insensitive to driving GCM. All RCMs agree on higher winds over
411 the British Isles and weaker winds over northern Europe, but notably the mountainous regions have either low or high
412 wind speeds depending on the model, which must relate to how wind speed is calculated there - it can be imagined that
413 the wind speed in a valley would be somewhat different to that at the top of a mountain. In terms of differences between
414 the two resolutions of CORDEX, some RCMs show increased wind speeds with higher resolution e.g. RACMO,
415 HIRHAM5, and others less so. Again, ensemble members of the same model give similar results.

416

417 Figure 2 (right column) shows the return period plots for WindXx for CMIP5 and both resolutions of CORDEX. All
418 models are shifted to have the same climatology of annual maximum wind for each grid cell, which goes some way to
419 adjusting for differences in sampling frequency, although there is evidence that the shape of the tails is also affected
420 for some models (Figure S8). The results for the common subset of CORDEX runs should at least be directly
421 comparable to each other. The British Isles are shown instead of Northern Europe, since they are particularly affected
422 by wind extremes, and for comparison with the results for the UPSCALE simulations, where this region shows



423 distinctive results. The distribution of annual maximum sfcWindmax has heavier tails in CORDEX 0.11 compared to
424 0.44 which is in turn heavier than CMIP5, regardless of the subset of models used in creating the pooled ensemble in
425 almost all regions examined. The CMIP5 results are somewhat sensitive to the models included. The model results
426 appear relatively consistent with the WFDEI and ECEM-noc observations (note the different sampling frequency).
427 ECEM-wbc is much heavier tailed in southern and Central Europe.

428

429 In summary, winds tend to be stronger, with heavier tails at higher resolution, with a large spread between models.
430 Observational datasets give very diverse results.

431

432 **4.2 Global high resolution: UPSCALE**

433 We now examine the benefits or otherwise of global high vs. standard resolution simulations for simulating climate
434 extremes. Global high resolution may allow an improved representation of the large scale circulation that cannot be
435 captured by regional models, which may in turn affect the representation of climate extremes. For this we examine the
436 UPSCALE simulations (Mizielinski et al. 2014), which consist of a small ensemble of HadGEM3-A simulations at
437 three different resolutions: 130km (N96), 60km (N216), and 25km (N512) (see Data section).

438 **4.2.1 Temperature extremes**

439 Figure 5 shows the ensemble mean climatological mean of TXx5day for the UPSCALE simulations over the period
440 1985-2011 at all three resolutions, and their biases relative to E-OBS. The same general pattern of hotter extremes in
441 the south and colder in the north and over mountainous regions can be seen at all three resolutions, but temperature
442 extremes are hotter at higher resolution in the south and east, and colder over mountains. The same pattern of biases is
443 seen as for CORDEX and CMIP5 with cold biases in the north and hot in the south-east and over mountains. The
444 mountain biases reduce with higher resolution, as the orography becomes better defined, whilst the hot bias in the SE
445 and SW increases and the northern cold bias improves slightly. A coastal cold bias at low resolution disappears at
446 higher resolution, presumably because the ocean influence is carried further over land at low resolution in the large
447 grid boxes. Note that the SSTs are prescribed and are the same for all simulations. Results for TXx are similar but
448 hotter (not shown).

449

450 Figure 6 (left column) shows regional return period plots for TXx5day for the UPSCALE simulations. Results are a
451 little less consistent across regions for UPSCALE compared to the CMIP5 vs CORDEX analysis, so we split Northern
452 Europe into the British Isles and Scandinavia, and add the Alps, to better capture regional variations. Again, the thin
453 lines are individual simulations, and the circles are for results pooled across the ensemble members for each resolution
454 separately. Since the pooled ensembles are only based on one model, results are presented without adjusting according
455 to the climatology of TXx5day, although bias adjusted results can be seen in Figure S11 and allow differences in the
456 shapes of the tails to be seen more clearly. TXx5day seems to be hotter with higher resolution over most regions, with
457 the notable exception of the Alps, where the higher elevations with higher resolution give rise to colder temperature



458 extremes. There are notable biases relative to the observations, with the models being too cold in the north, especially
459 at low resolution, whilst in the south the colder subset of models (N96, the lowest UPSCALE resolution) agree with
460 the observations. Over the Alps, again the low resolution simulations agree best with observations, with the warmest
461 temperatures, but this will depend on the height of the meteorological stations. This apparent contradiction to the
462 reduced orographic hot bias with resolution in figure 5 comes from the stronger cold bias of the surrounding areas at
463 low resolution. Figure S11 shows that in general there is not much difference between the shape of the tails with
464 resolution, with only slightly heavier tails with increased resolution over the British Isles and Southern Europe.
465 Agreement with E-OBS is very good everywhere. Results for TXx are similar.

466

467 In summary, hot biases of temperature extremes over mountains reduce with increased resolution for HadGEM3-A.
468 Elsewhere extremes get hotter with resolution, whilst the shapes of the statistical distributions are insensitive.

469 **4.2.2 Precipitation extremes**

470 For precipitation, Figure 7 shows the ensemble mean climatological mean of Rx1day for the period 1989-2010 for the
471 three UPSCALE ensembles and their biases relative to E-OBS. The overall pattern of Rx1day is similar to that in E-
472 OBS, with heavier precipitation extremes and finer spatial detail with increasing resolution over complex orography.
473 The N96 runs have an area of heavy precipitation stretching from France into Germany, whilst the N216 and N512
474 simulations show instead a pattern of heavy precipitation either side of the Alps, with a drier area in-between. A general
475 wet bias can be seen at all resolutions over Europe, whilst the dry bias over orography in the Alps, Southern Norway
476 and Scottish Highlands reduces with resolution and a wet bias on the southern edge of the Alps and the coastal side of
477 the Dinaric Alps in the Balkans appears as resolution increases. Comparing to MESAN instead of E-OBS, the general
478 wet bias disappears, and the dry mountain bias over orography at low resolution increases. The differences between
479 resolutions appear smaller than for the CMIP5 versus CORDEX analysis: all the UPSCALE simulations look most
480 similar to CORDEX at 0.44°. However, UPSCALE does not reach as fine a resolution as CORDEX at 0.11° (25 km
481 vs 12.5 km), and CMIP5 is on average slightly coarser than the N96 simulations. In addition, it should be noted that a
482 model's nominal resolution does not always accurately reflect the spatial scales that it can represent. Results are similar
483 for Rx5day (not shown).

484

485 Figure 6 (middle column) shows the return period plots for Rx1day for the three resolutions of UPSCALE ensembles.
486 Slightly heavier precipitation extremes are found at higher resolution in all the regions shown (exceptions are France
487 and Mid Europe- not shown), although differences are small, they are more obvious in southern Europe and especially
488 in the Alps. Figure S11 shows that there is not much difference in the shape of the tails for most regions, although
489 there are very slightly heavier tails at higher resolution for southern Europe and more obvious differences over the
490 Alps in the same direction, both of which are regions where convective precipitation is important. E-OBS tends to lie
491 just below the model simulations for most regions (Figure 6 – compare with the thin coloured lines), although it agrees
492 with the models for the British Isles, and is between the low and medium resolution simulations over the Alps. MESAN
493 gives higher values for observed Rx1day which improves agreement in regions where E-OBS lay below the models,



494 and causes a higher resolution subset to agree better in the other regions (Figure 6). For the bias adjusted versions E-
495 OBS tends to lie just on the lower end of the ensemble for most regions, whilst MESAN gives slightly heavier tails
496 and tends to improve agreement with models (Figure S11). Results for Rx5day are broadly similar (except that both
497 sets of observations lie above all the models for the British Isles).

498

499 In summary, precipitation extremes are somewhat wetter and heavier tailed with increasing resolution mostly in
500 southern Europe and the Alps for HadGEM3-A. Dry orographic biases decrease with resolution but wet biases appear
501 in the south next to mountain ranges instead.

502 **4.2.3 Wind extremes**

503 For wind extremes, Figure 8 shows the spatial patterns of climatological mean annual maximum wind based on 6-
504 hourly data for UPSCALE and the same for three observational datasets. In this case the models and observations are
505 directly comparable since they share the same temporal resolution. The spatial patterns are similar for the three
506 different model resolutions, with the highest winds over the British Isles and coastal regions, lower wind speeds over
507 the Alps, and the zonal tripole pattern described above, although this does not extend as far east as in the observations
508 (i.e. ECEM-noc and WFDEI). The main differences are that the lower resolution model (N96) has stronger winds
509 around the British Isles and western coastlines, presumably because the larger grid boxes overlap more with the ocean,
510 which tends to have higher wind speeds. The wind speeds at higher resolution are a little stronger overall, most
511 obviously in the central European zonal belt, and over the Alps and Norwegian mountains. As noted before, the
512 observational estimates vary significantly and therefore the biases depend on the observational dataset used, i.e.
513 extreme winds are slightly weak compared to ECEM-noc over much of Europe; compared to WFDEI, winds are too
514 strong in the north and south, and too weak in the east; and compared to ECEM-wbc, winds are far too weak in the
515 north and south and too strong in-between.

516

517 Figure 6 (right column) shows the return period plots for annual maximum wind for the UPSCALE simulations,
518 without shifting the climatology. Over most regions the strongest extreme winds are found at the highest resolution,
519 with the exception of the British Isles (and the Iberian Peninsula- not shown) where the low resolution models have
520 the strongest winds. This is likely related to the large coastal grid boxes overlapping windy ocean areas as discussed
521 above. As noted above, there are large differences between observational estimates, with ECEM-wbc having
522 considerably higher values and heavier tails than the other two datasets and models over most regions, except the
523 British Isles. ECEM-noc tends to agree best with the model simulations, whilst WFDEI tends to lie at the lower end of
524 the model range or underneath. For the bias adjusted versions of the return period plots (Figure S11), differences in
525 the shapes of the tails with resolution are generally small, although with marginally heavier tails with increasing
526 resolution over a number of regions. Agreement of the shape of the tails with ECEM-noc and WFDEI is good.

527

528 In summary winds are slightly stronger and heavier tailed at higher resolution in HadGEM3-A, except over coastal
529 areas where large grid boxes at low resolution bring strong ocean winds further over land.



530 4.3 Circulation Analogues

531 For the global model results, any differences in the representation of extremes according to resolution could come from
532 either upscaling or downscaling effects. Upscaling effects could include a better representation of the large scale
533 circulation, whilst downscaling allows a better representation of small scale processes, such as convection, and an
534 improved representation of orography and coastlines. In order to investigate which of these effects leads to the
535 differences between the low (N96) and high resolution (N512) HadGEM3-A simulations, we employ a circulation
536 analogue technique (e.g. Vautard et al., 2016), which is frequently used in attribution studies (see e.g. Stott et al., 2016;
537 Cattiaux et al., 2010). The idea is to determine whether the simulation of climate extremes changes between the two
538 resolutions if both were to have the same large scale circulation –i.e. isolating the downscaling effect, or conversely
539 whether circulation differences explain any differences in extreme events whilst circulation-variable (e.g. precipitation)
540 relationships stay the same –i.e. the upscaling effect.

541

542 For each day in the lower resolution simulations we pick the nearest circulation analogue from anywhere in the higher
543 resolution simulations, providing it happens at the right time of year (i.e. within a 30-day window centred on the day
544 of the year in question). We then record the associated temperature, precipitation and wind values from the higher
545 resolution simulations to make a “u-chronic” dataset (e.g. Jézéquel, et al. 2018) that contains data from the high
546 resolution simulations but follows the daily sequence of circulation patterns from the low resolution models. We then
547 repeat the analysis of return periods and value as above. We also do the reverse (find analogues for the N512 circulation
548 in the N96 ensemble and record the N96 temperature). Since results using analogues are not directly comparable to the
549 original results, due to lack of exact analogue match, we also perform “self-analogues” -i.e. finding circulation
550 analogues for the N96 simulations within the N96 ensemble, (excluding the same year from the same ensemble
551 member) and creating a u-chronic time series, and the same for the N512 ensemble). Comparing the resulting return
552 period curves tells us about the contribution of large-scale circulation and downscaling to differences in extremes
553 between the two resolutions. For example, comparing the N96 self-analogue return curve to the version based on N512
554 circulation but with N96 precipitation shows us the contribution of any differences in the large scale circulation
555 between the resolutions i.e. the upscaling effect. Comparing the N96 self-analogue to the version based on N96
556 circulation with N512 precipitation shows us the downscaling effect – i.e. any difference between the relationship
557 between the large scale circulation and precipitation.

558

559 Analogues are defined using geopotential height at 500 hpa, since this avoids complications relating to surface heat
560 lows associated with heat waves in anticyclonic conditions that occur in summer, whilst also avoiding incomplete data
561 due to mountain ranges. Geopotential height is regridded to a 2° grid using bilinear interpolation. This choice ensures
562 that we are comparing analogues with the same resolution and do not penalise small-scale differences. Similarity
563 between circulation states is calculated using the Euclidean distance. For precipitation and wind the European domain
564 used is -16 to 44° E and 34 to 72° N (roughly the same as the domain plotted in the map-based figures). For temperature,
565 a larger domain is used, since the history and trajectory of air masses is important for temperature extremes. This
566 domain is loosely based on the domain used by Cattiaux et al. (2010) and extends over the N. Atlantic as well as



567 Europe, (-62 to 44°E and 24 to 80° N). However, results are very similar if the smaller domain is used (not shown).
568 For the 5-day variables (Rx5day and TXx5day); daily geopotential height, precipitation and temperature datasets were
569 smoothed using a 5-day running mean first, and then analogues were calculated, and the u-chronic datasets constructed.
570 We also tried doing the 5-day means last rather than first, i.e. calculating analogues using daily data and smoothing
571 the u-chronic dataset. The relationship between the different curves was largely consistent between the two techniques,
572 but absolute values differed and the shape of the distributions changed a little. Results presented here are based on the
573 first technique since it replicates better the autocorrelation structure of the original analysis.

574
575 Figure 9 shows the results of the analogue analysis. The blue curves show the results for the N512 self-analogues, grey
576 represents the N96 self-analogues, red represents results using the circulation patterns from the N96 runs but with the
577 N512 circulation-variable relationships, and green indicates N512 circulation with N96 circulation-variable
578 relationships. The difference between the blue and red curves (or the grey and green curves) shows the contribution
579 from differences in the large scale circulation with resolution, whilst the difference between the blue and green curves
580 (or the red and grey curves) indicates the downscaling effect.

581
582 For TXx5day downscaling effects are dominant over regions that have a clear difference between resolutions, although
583 circulation differences also have a small effect in some regions (Figure 9). For Rx1day the different curves are very
584 close together for most regions, making it difficult to discern the relative contributions from upscaling and
585 downscaling. However, it generally seems to be downscaling effects that are the most important, and this can be seen
586 more clearly for the Alps and Southern Europe where there are larger differences with resolution. Interestingly, these
587 are regions where convective precipitation is particularly important for precipitation extremes. For wind extremes
588 downscaling effects also dominate, but the large scale circulation also plays a role in Scandinavia. Results for TXx and
589 Rx5day are very similar to those for TXx5day and Rx1day respectively (not shown).

590
591 Also shown, using thick solid lines, are the original pooled ensemble results without using analogues. By comparing
592 these with the self-analogue results (i.e. compare the blue line with the blue circles for N512, and the grey line with
593 the grey circles for N96), we can see how successful the analogue technique is in recreating the original distributions.
594 The self-analogue results tend to be close to, but slightly below the original results for wind and Rx1day, with a slight
595 difference in the shape of the tail at the far right for Rx1day. This can be explained by the fact that the analogues are
596 not perfect, and since the circulation patterns associated with climate extremes are rare, the nearest analogues are likely
597 to represent slightly less severe events. The original results are beneath the analogue results and a different shape for
598 TXx5day, which seems to be associated with the 5-day averaging, and is much less marked for TXx (not shown).
599 Undertaking the 5-day averaging last rather than first (see Methods) shifts analogue results downwards, underneath
600 the original curves, but otherwise gives the same results (not shown). The same phenomenon is seen for Rx5day (not
601 shown).

602



603 In summary, for all three types of extreme events, downscaling effects appear to dominate the differences seen between
604 the 130km and 25km HadGEM3-A simulations. This suggests that at least for this model, any large scale circulation
605 differences obtained with global high resolution do not affect the statistics of these extreme events much.

606 **5 Summary and Discussion**

607 **5.1 Summary**

608 We evaluated climate model simulations of temperature, precipitation and wind extremes over Europe, addressing
609 three questions: 1) The benefits of dynamical downscaling using regional climate models by comparing EURO-
610 CORDEX simulations at two resolutions (12.5 and 50 km) to their driving coarser resolution CMIP5 models; 2) The
611 benefits of increased resolution for global models by comparing HadGEM3-A simulations at three resolutions (130,
612 60 and 25 km); and 3) whether any differences according to resolution in the global model comes from differences in
613 the large scale circulation (upscaling) or the representation of small scale processes, and features (downscaling) using
614 a circulation analogue method.

615

616 For temperature extremes, increased resolution did not make much difference to results for the CORDEX vs CMIP5
617 analysis, both in terms of the shapes of the distributions, which all agreed well with observations, or in terms of biases,
618 apart from reducing hot biases over mountains. This reduction in orographic bias with increased resolution was also
619 seen in the HadGEM3-A GCM simulations, along with a general increase in magnitude of hot extremes elsewhere,
620 which reduces biases in the north, and increases them in the south. Overall the benefits of increasing resolution were
621 limited, or region dependent.

622

623 Precipitation extremes were more sensitive to resolution, particularly in the CMIP5 vs CORDEX analysis, with heavier
624 tails at higher resolution across all regions. Spatially, CMIP5 shows a general dry bias compared to E-OBS, particularly
625 over mountainous regions, whilst CORDEX shows the opposite, with increasing wet biases at 0.11° compared to 0.44° ,
626 which appears to be systematic across models. The higher resolution MESAN reanalysis gave wetter extremes and
627 heavier tails than E-OBS, agreeing best with the 0.44° resolution CORDEX simulations, highlighting the importance
628 of the choice of observational dataset. Differences according to resolution were smaller for the global scale HadGEM3-
629 A simulations, although these span a smaller range of resolutions. Differences were most obvious in southern regions
630 and the Alps, with heavier tails and wetter extremes at higher resolution. Dry biases over orography decreased with
631 increasing resolution; however, wet biases next to some mountain ranges in the south emerge. Return period curves
632 for HadGEM3-A tended to agree well with MESAN, but were too wet compared to E-OBS.

633

634 For wind extremes, higher resolution gave stronger winds and heavier tails for most regions for both the CORDEX vs
635 CMIP5 analysis and to a lesser extent for HadGEM3-A. The largest differences were between CMIP5 and CORDEX
636 at 0.44° , with less difference between the two resolutions of CORDEX. Differences between observational estimates



637 made model evaluation difficult, whilst inconsistencies in the way daily maximum wind is calculated in different
638 models were also an issue.

639

640 The circulation analogue analysis suggested that for the global scale HadGEM3-A simulations, differences according
641 to resolution for all three phenomena were dominated by downscaling effects, with only small contributions from
642 differences in the large-scale circulation.

643

644 **5.2 Discussion**

645 For temperature extremes, our results imply that increased resolution in both regional and global models is of limited
646 benefit at the resolution range considered here, except in reducing the hot bias over mountainous areas. In particular,
647 for resolutions used in the UPSCALE experiments, we do not find strong upscaling nor downscaling effects. These
648 findings agree with Vautard et al. (2013) for regional models, who find limited benefits in simulating various aspects
649 of heatwaves between the 0.44° and 0.11° versions of the EURO-CORDEX models. However, our results for the
650 global model analysis are based on only one model and the new model simulations and analyses being generated as
651 part of the PRIMAVERA and HighResMIP projects (<https://www.primavera-h2020.eu/>; Roberts et al. 2018; Haarsma
652 et al. 2016) will be very useful for determining how representative our results for HadGEM3-A are of other GCMs.
653 For instance, improvements in the simulation of summer blocking, which can be involved in heatwave generation is
654 very model dependent (Scheimann et al. 2014). Furthermore, Cattiaux et al. (2013) find that the frequency, intensity
655 and duration of summer heatwaves improve in the IPSL model with resolution, associated with a better representation
656 of the large scale circulation. In addition, here we examine only one aspect of heat waves (intensity), and it could be
657 that results are different for others aspects, such as frequency, duration and timing.

658

659 For precipitation extremes, we found that the CMIP5 models were too dry whilst CORDEX was a little too wet at
660 0.44° and more so at 0.11° when compared to E-OBS. This was particularly the case over complex orography. This is
661 consistent with results for mean precipitation in EURO-CORDEX in Kotlarski et al. (2014). However, our results
662 depend on the observational dataset compared against, with MESAN giving heavier extremes than E-OBS and agreeing
663 reasonably well with the 0.44° simulations. Other studies suggest that country-scale higher resolution precipitation
664 datasets give heavier precipitation extremes still, which may agree best with the 0.11° simulations. Similarly, for mean
665 precipitation, Prein and Gobeit (2017) find that RCM biases are a similar size to the differences between different
666 observational estimates. For extreme precipitation, Prein et al (2016) and Torma et al (2015) find that various aspects
667 (biases, frequency-intensity distributions, spatial patterns) of mean and extreme precipitation improve in EURO-
668 CORDEX at 0.11° compared to 0.44° when compared to such datasets for Europe and the Alps respectively. Prein et
669 al (2016) ascribe this mostly to the better representation of orography at higher resolution, but also the ability to capture
670 the larger scales of convection. However, some of the difference in our results may also be explained by
671 parameterisation schemes that tend to be tuned to one resolution and can behave sub-optimally at others.



672 For the UPSCALE global simulations, there was less difference with resolution, with the biggest differences over or
673 near mountains. However, these simulations span a narrower range of resolutions, i.e. not reaching the same high
674 resolutions as CORDEX 0.11°, but also not as coarse as some CMIP5 models. Other global model studies also tend to
675 find an increase in precipitation extremes with increased resolution for Europe, which is continent-wide in summer,
676 and concentrated in mountainous regions in winter (Volosciuk et al. 2015; Wehner et al. 2014). This sometimes
677 improves agreement with observations (e.g. Koppala et al. 2013; Wehner et al. 2014 for winter), but can overestimate
678 summer extreme precipitation if parameterisation schemes are not retuned (Wehner et al. 2014).

679

680 For wind extremes, our findings of stronger winds and heavier tails with increased resolution are consistent with
681 previous studies (e.g. Pryor et al. 2012; Champion et al. 2011; Kunz et al. 2010). However, observational issues made
682 model evaluation difficult.

683

684 The results of the circulation analogue analysis on the HadGEM3-A GCM simulations suggested that downscaling
685 effects were the dominant cause of differences with resolution for all three phenomena, with limited effects of any
686 differences in the representation of the large scale circulation. If this result also applied to other GCMs, it would suggest
687 that dynamical downscaling with more economical limited area models would be a better strategy for simulating
688 European extreme events, whilst GCM efforts could focus on other aspects such as multiple members or multi-physics
689 ensembles. However, we cannot reach this conclusion based solely on this analysis, since we examine only a single
690 model, which may not be representative of other models, and because the range of resolutions considered may be too
691 narrow. Furthermore, a number of studies do find improvements in the large-scale circulation with resolution, including
692 for extra-tropical cyclones and storm tracks (Colle et al. 2013; Jung et al 2006; 2012, Zappa et al. 2013), Euro-Atlantic
693 weather regimes (Dawson et al. 2012; 2015; Cattiaux et al. 2013) and blocking (Jung et al. 2012, Anstey et al. 2013;
694 Matsueda et al. 2009, Berckmans et al 2013; Scheimann et al. 2014; Davini et al 2017a; 2017b; see also Introduction).
695 Interestingly, Scheimann et al. (2017) find improvements in Euro-Atlantic blocking with resolution in all seasons in
696 the same HadGEM3-A simulations as we analyse here. However, the net effects on extremes, given all uncertainties,
697 was not explicitly investigated. Our study does not seem to be able to discern such effects.

698

699 Overall our results suggest that whether or not increased resolution is beneficial for the simulation of extreme events
700 over Europe depends on the event being considered. Benefits appear limited for heatwaves, whereas wind extremes
701 and particularly precipitation extremes are more sensitive. We do not find any particular advantage in using a global
702 high resolution model compared to regional dynamical downscaling, with the caveats that this investigation needs to
703 be extended to other GCMs, and a wider range of resolutions should be investigated.

704

705 In order to fully address the question of the benefits of increased resolution for European climate extremes, a number
706 of aspects remain to be investigated. Firstly, the analysis could be widened to other types of extremes, for example,
707 sea level rise and storm surge, or other aspects of extremes could be considered e.g. timing, frequency and duration of
708 events. The global simulations we investigated were atmosphere-only, and the role of increased ocean resolution and
709 also vertical resolution and model top height should be considered. Finally, we assume that better historical



710 performance translates into more accurate future projections. Lhotka et al. (2018) find low sensitivity of heatwave
711 projections to resolution in EURO-CORDEX RCMs. However, Van Haren et al. (2015b) find stronger future summer
712 drying and heating in central Europe with increased resolution in the EC-Earth GCM due to differences in atmospheric
713 circulation. Concerning precipitation, future projections for large scale and seasonal mean precipitation are consistent
714 between large scale and convective permitting models, whereas summer daily and sub-daily intensities increase more
715 in the future in convection permitting models (Kendon et al. 2017; Ban et al. 2015; Kendon et al. 2014). For wind,
716 Willison et al. (2015) find a larger response of the North Atlantic storm track to global warming with higher resolution
717 in the WRF model. The sensitivity of projections to resolution nevertheless remains an area that needs further research.

718 **Data and code availability**

719 The CMIP5 and CORDEX data used for this analysis are available from the Earth System Grid Federation portals, and
720 are detailed in Table S1. The HadGEM3-A UPSCALE simulations are available from the CEDA-JASMIN platform.
721 E-OBS can be downloaded here <https://www.ecad.eu/download/ensembles/download.php>, MESAN is available here
722 <http://exporter.nsc.liu.se/620eed0cb2c74c859f7d6db81742e114/>, access to WFDEI is detailed here [http://www.eu-watch.org/gfx_content/documents/README-WFDEI%20\(v2016\).pdf](http://www.eu-watch.org/gfx_content/documents/README-WFDEI%20(v2016).pdf) and ECEM data are available from the
723 Copernicus Climate Data Store <https://cds.climate.copernicus.eu>.
724

725 **Author contributions**

726 CI, RV and SJ conceptualised the study, CI carried out the analysis and wrote the manuscript, JS managed the CRECP
727 project together with CH and BE, and all co-authors were involved in discussions to prepare the study and helped
728 improve the manuscript.

729 **Competing interests**

730 The authors declare that they have no conflict of interest.

731 **Acknowledgements**

732 This work is published in the name of the European Commission, with funding from the European Union through the
733 Copernicus Climate Change Service project C3S_34a Lot 3 (Copernicus Roadmap for European Climate Projections).
734 The Commission is not responsible for any use that may be made of the information contained. We acknowledge the
735 WCRP's Working Group on Regional Climate, and the Working Group on Coupled Modelling - the coordinating body
736 of CORDEX and the panel responsible for CMIP5 respectively. We thank the climate modelling groups for producing
737 and making available the model output listed in Supplementary Table 1, which is available at <http://pcmdi9.llnl.gov>.
738 For CMIP, the US Department of Energy's Program for Climate Model Diagnosis and Intercomparison provides
739 coordinating support and led development of software infrastructure in partnership with the Global Organization for
740 Earth System Science Portals. We thank the modelling team that produced the UPSCALE simulations, and



741 acknowledge the JASMIN and IPSL mesocentre computing clusters on which this analysis was performed. We also
742 acknowledge helpful input from the CRECP project scientific advisory board and useful discussions with UK Met
743 Office Scientists, in particular Malcolm Roberts and Carol McSweeney.

744

745 **References**

746 Anstey, J. A., Davini, P., Gray, L. J., Woollings, T. J., Butchart, N., Cagnazzo, C., Christiansen, B., Hardiman, S. C.,
747 Osprey, S. M. and Yang, S.: Multi- model analysis of Northern Hemisphere winter blocking: Model biases and the
748 role of resolution, *J. Geophys. Res. Atmos.*, 118, 3956–3971, doi: 10.1002/jgrd.50231, 2013.

749

750 Ban, N., Schmidli, J. and Schär, C.: Heavy precipitation in a changing climate: Does short- term summer precipitation
751 increase faster?, *Geophys. Res. Lett.*, 42, 1165–1172, doi: 10.1002/2014GL062588, 2015.

752

753 Berckmans, J., Woollings, T., Demory, M. E., Vidale, P.-L. and Roberts, M.: Atmospheric blocking in a high resolution
754 climate model: influences of mean state, orography and eddy forcing, *Atmos. Sci. Lett.*, 14, 34–40,
755 doi:10.1002/asl2.412, 2013.

756

757 Cattiaux, J., Vautard, R., Cassou, C., Yiou, P., Masson-Delmotte, V., and Codron, F.: Winter 2010 in Europe: A cold
758 extreme in a warming climate, *Geophys. Res. Lett.*, 37, L20704, doi: 10.1029/2010GL044613, 2010.

759

760 Cattiaux, J., Quesada, B., Arakélian, A., Codron, F., Vautard, R., Yiou, P.: North-Atlantic dynamics and European
761 temperature extremes in the IPSL model: sensitivity to atmospheric resolution, *Clim. Dynam.*, 40, 2293– 2310,
762 doi:10.1007/s00382-012-1529-3, 2013.

763

764 Champion, A. J., Hodges, K. I., Bengtsson, L. O., Keenlyside, N. S. and Esch, M.: Impact of increasing resolution and
765 a warmer climate on extreme weather from Northern Hemisphere extratropical cyclones, *Tellus A*, 63, 893-906,
766 doi:10.1111/j.1600-0870.2011.00538.x, 2011.

767

768 Christensen, J. H. and Christensen, O. B.: A summary of the PRUDENCE model projections of changes in European
769 climate by the end of this century, *Climatic Change*, 81, 7–30, doi: 10.1007/s10584-006-9210-7, 2007.

770

771 Colle, B. A., Zhang, Z., Lombardo, K., Liu, P., Chang, E. and Zhang, M.: Historical evaluation and future prediction
772 in Eastern North America and western Atlantic extratropical cyclones in the CMIP5 models during the cool season, *J.*
773 *Climate.*, 26, 882–903, doi: 10.1175/JCLI-D-12-00498.1, 2013.

774

775 Coppola, E., Sobolowski, S., Pichelli, E., Raffaele, F., Ahrens, B., Anders, I., Ban, N., Bastin, S., Belda, M., Belusic,
776 D., Caldas-Alvarez, A., Margarida Cardoso, R., Davolio, S., Dobler, A., Fernandez, J., Fita Borrell, L., Fumiere, Q.,



777 Giorgi, F., Goergen, K., Guettler, I., Halenka, T., Heinzeller, D., Hodnebrog, Ø., Jacob, D., Kartsios, S., Katragko, E.,
778 Kendon, E., Khodayar, S., Kunstmann, H., Knist, S., Lavín, A., Lind, P., Lorenz, T., Maraun, D., Marelle, L., van
779 Meijgaard, E., Milovac, J., Myhre, G., Panitz, H.-J., Piazza, M., Raffa, M., Raub, T., Rockel, B., Schär, C., Sieck, K.,
780 Soares, P. M. M., Somot, S., Srnec, L., Stocchi, P., Tölle, M., Truhetz, H., Vautard, R., de Vries, H. and Warrach-Sagi,
781 K.: A first-of-its-kind multi-model convection permitting ensemble for investigating convective phenomena over
782 Europe and the Mediterranean, *Clim. Dynam.*, 1-32, <https://doi.org/10.1007/s00382-018-4521-8>, 2018.

783

784 Dahlgren, P., Landelius, T., Kållberg, P. and Gollvik, S., A high- resolution regional reanalysis for Europe. Part 1:
785 Three- dimensional reanalysis with the regional HIgh- Resolution Limited- Area Model (HIRLAM), *Q.J.R.*
786 *Meteorol. Soc.*, 142, 2119-2131, doi:10.1002/qj.2807, 2016

787

788 Davini, P., Corti, S., D'Andrea, F., Rivière, G., and von Hardenberg, J.: Improved Winter European Atmospheric
789 Blocking Frequencies in High- Resolution Global Climate Simulations. *J. Adv. Model. Earth Syst.*, 9, 2615–2634,
790 <https://doi.org/10.1002/2017MS001082>, 2017a.

791

792 Davini, P., von Hardenberg, J., Corti, S., Christensen, H. M., Juricke, S., Subramanian, A., Watson, P. A. G.,
793 Weisheimer, A., and Palmer, T. N.: Climate SPHINX: evaluating the impact of resolution and stochastic physics
794 parameterisations in the EC-Earth global climate model, *Geosci. Model Dev.*, 10, 1383-1402,
795 <https://doi.org/10.5194/gmd-10-1383-2017>, 2017b.

796

797 Dawson, A. and Palmer, T. N.: Simulating weather regimes: impact of model resolution and stochastic
798 parameterization. *Clim Dynam*, 44, 2177-2193, <https://doi.org/10.1007/s00382-014-2238-x>, 2015.

799

800 Dawson, A., Palmer, T. N., and Corti, S.: Simulating regime structures in weather and climate prediction models,
801 *Geophys. Res. Lett*, 39, L21805, <https://doi.org/10.1029/2012GL053284>, 2012.

802

803 Dee, D. P., Uppala, S. M., Simmons, A. J, Berrisford, P., Poli, P., Kobayashi, S., Andrae, U., Balmaseda, M. A.,
804 Balsamo, G., Bauer, P., Bechtold, P., Beljaars, A. C., van de Berg, L., Bidlot, J., Bormann, N., Delsol, C., Dragani, R.,
805 Fuentes, M., Geer, A. J., Haimberger, L., Healy, S. B., Hersbach, H., Hólm, E. V., Isaksen, L., Kållberg, P., Köhler,
806 M., Matricardi, M., McNally, A. P., Monge- Sanz, B. M., Morcrette, J., Park, B., Peubey, C., de Rosnay, P., Tavolato,
807 C., Thépaut, J. and Vitart, F.: The ERA-Interim reanalysis: Configuration and performance of the data assimilation
808 system, *Q. J. R. Meteorol. Soc.*, 137, 553–597, <https://doi.org/10.1002/qj.828>, 2011.

809

810 Demory, M. E., Vidale, P. L., Roberts, M. J., Berrisford, P., Strachan, J., Schiemann, R., and Mizielinski, M. S.: The
811 role of horizontal resolution in simulating drivers of the global hydrological cycle, *Clim. Dynam.*, 42, 2201–2225,
812 <https://doi.org/10.1007/s00382-013-1924-4>, 2014.

813



- 814 Donat M. G., Leckebusch G. C., Wild S., Ulbrich U.: Benefits and limitations of regional multi-model ensembles for
815 storm loss estimations, *Clim. Res.*, 44, 211-225. <https://doi.org/10.3354/cr00891>, 2010.
- 816
- 817 Dunn, R. J. H., Willett, K. M., Thorne, P., Woolley, E. V., Durre, I., Dai, A., Parker, D. E., Vose, R. S.: HadISD: A
818 Quality Controlled global synoptic report database for selected variables at long-term stations from 1973-2011, *Clim.*
819 *Past*, 8, 1649-1679, doi: 10.5194/cp-8-1649-2012, 2012.
- 820
- 821 Førland, E. and Institut, N. M.: Manual for Operational Correction of Nordic Precipitation Data. Norwegian
822 Meteorological Institute., 1996.
- 823
- 824 Giorgi F., Jones C., Asrar G. R.: Addressing climate information needs at the regional level: the CORDEX framework,
825 *WMO Bull.*, 58:175–183, 2009.
- 826
- 827 Goodison, B. E., Louie, P. Y. and Yang, D.: The WMO solid precipitation measurement intercomparison. World
828 Meteorological Organization-Publications-WMO TD, Report No. 67, 65–70, 1997.
- 829
- 830 Gutjahr, O., Schefczyk, L., Reiter, P. and Heinemann, G.: Impact of the horizontal resolution on the simulation of
831 extremes in COSMO-CLM, *Meteorol. Z.*, 25, 543 – 562, doi: 10.1127/metz/2016/0638, 2016.
- 832
- 833 Haarsma, R. J., Roberts, M. J., Vidale, P. L., Senior, C. A., Bellucci, A., Bao, Q., Chang, P., Corti, S., Fuckar, N. S.,
834 Guemas, V., von Hardenberg, J., Hazeleger, W., Kodama, C., Koenigk, T., Leung, L. R., Lu, J., Luo, J.-J., Mao, J.,
835 Mizielinski, M. S., Mizuta, R., Nobre, P., Satoh, M., Scoccimarro, E., Semmler, T., Small, J., and von Storch, J.-S.:
836 High Resolution Model Intercomparison Project (HighResMIP v1.0) for CMIP6, *Geosci. Model Dev.*, 9, 4185-4208,
837 <https://doi.org/10.5194/gmd-9-4185-2016>, 2016.
- 838
- 839 Haylock, M. R., Hofstra, N., Klein Tank, A. M. G., Klok, E. J., Jones, P. D., New, M.: A European daily high-resolution
840 gridded data set of surface temperature and precipitation for 1950-2006. *J. Geophys. Res. Atmos.*, 113, D20119.
841 doi:10.1029/2008JD010201, 2008.
- 842
- 843 Herrmann, M., Somot, S., Calmanti, S., Dubois, C., and Sevault, F.: Representation of spatial and temporal variability
844 of daily wind speed and of intense wind events over the Mediterranean Sea using dynamical downscaling: impact of
845 the regional climate model configuration, *Nat. Hazards Earth Syst. Sci.*, 11, 1983-2001, [https://doi.org/10.5194/nhess-](https://doi.org/10.5194/nhess-11-1983-2011)
846 [11-1983-2011](https://doi.org/10.5194/nhess-11-1983-2011), 2011.
- 847
- 848 Jacob, D., Petersen, J., Eggert, B., Alias, A., Christensen, O. B., Bouwer, L. M., Braun, A., Colette, A., Déqué, M.,
849 Georgievski, G., Georgopoulou, E., Gobiet, A., Menut, L., Nikulin, G., Haensler, A., Hempelmann, N., Jones, C.,
850 Keuler, K., Ko-vats, S., Kröner, N., Kotlarski, S., Kriegsmann, A., Martin, E., Meijgaard, E. van, Moseley, C., Pfeifer,
851 S., Preuschmann, S., Radermacher, C., Radtke, K., Rechid, D., Rounsevell, M., Samuelsson, P., Somot, S., Soussana,



852 J.-F., Teichmann, C., Valentini, R., Vautard, R., Weber, B., and Yiou, P.: EURO-CORDEX: new high-resolution
853 climate change projections for European impact research, *Reg. Environ. Change*, 14, 563–578, doi:10.1007/s10113-
854 013-0499-2, 2014.

855

856 Jézéquel, A., Yiou, P. and Radanovics, S.: Role of circulation in European heatwaves using flow analogues. *Clim.*
857 *Dynam.* 50, 1145-1159, <https://doi.org/10.1007/s00382-017-3667-0>, 2018.

858

859 Jones, P. D., Harpham, C., Troccoli, A., Gschwind, B., Ranchin, T., Wald, L., Goodess, C. M., and Dorling, S. Using
860 ERA-Interim reanalysis for creating datasets of energy-relevant climate variables, *Earth Syst. Sci. Data*, 9, 471-495,
861 <https://doi.org/10.5194/essd-9-471-2017>, 2017.

862

863 Jung, T., Gulev, S. K., Rudeva, I. and Soloviov, V.: Sensitivity of extratropical cyclone characteristics to horizontal
864 resolution in the ECMWF model. *Q.J.R. Meteorol. Soc.*, 132, 1839-1857, doi:10.1256/qj.05.212, 2006.

865

866 Jung, T., Miller, M. J., Palmer, T. N., Towers, P., Wedi, N., Achuthavarier, D., Adams, J. M., Altshuler, E. L., Cash,
867 B. A., Kinter, J. L., Marx, L., Stan, C., and Hodges, K. I.: High-Resolution Global Climate Simulations with the
868 ECMWF Model in Project Athena: Experimental Design, Model Climate, and Seasonal Forecast Skill, *J. Climate.*, 25,
869 3155–3172, doi:10.1175/JCLI-D-11-00265.1, 2012.

870

871 Kendon, E. J., Roberts, N. M., Senior, C. A., and Roberts, M. J.: Realism of rainfall in a very high-resolution regional
872 climate model, *J. Climate.*, 25, 5791–5806. doi: 10.1175/JCLI-D-11-00562.1, 2012.

873

874 Kendon, E. J., Roberts, N. M., Fowler, H. J., Roberts, M. J., Chan, S. C., and Senior, C. A.: Heavier summer downpours
875 with climate change revealed by weather forecast resolution model, *Nat. Clim. Change*, 4, 570–576, doi:
876 10.1038/nclimate2258, 2014.

877

878 Kendon, E. J., Ban, N., Roberts, N. M., Fowler, H. J., Roberts, M. J., Chan, S. C., Evans, J. P., Fosser, G. and
879 Wilkinson, J.M.: Do Convection-Permitting Regional Climate Models Improve Projections of Future Precipitation
880 Change?. *B. Am. Meteorol. Soc.*, 98, 79–93, <https://doi.org/10.1175/BAMS-D-15-0004.1>, 2017.

881

882 Kopparla, P., Fischer, E. M., Hannay, C., and Knutti, R.: Improved simulation of extreme precipitation in a high-
883 resolution atmosphere model, *Geophys. Res. Lett.*, 40, 5803- 5808, doi: 10.1002/2013GL057866, 2013.

884

885 Kunz, M., Mohr, S., Rauthe, M., Lux, R., and Kottmeier, C.: Assessment of extreme wind speeds from Regional
886 Climate Models – Part I: Estimation of return values and their evaluation, *Nat. Hazards Earth Syst. Sci.*, 10, 907-922,
887 <https://doi.org/10.5194/nhess-10-907-2010>, 2010.

888



- 889 Landelius, T., Dahlgren, P., Gollvik, S., Jansson, A. and Olsson, E.: A high-resolution regional reanalysis for Europe.
890 Part 2: 2D analysis of surface temperature, precipitation and wind, *Q. J. R. Meteorol. Soc.*, 142, 2132–2142,
891 doi:10.1002/qj.2813, 2016.
- 892
- 893 Lhotka, O., Kyselý, J. and Farda, A.: Climate change scenarios of heat waves in Central Europe and their uncertainties.
894 *Theor Appl Climatol.*, 131, 1043–1054, <https://doi.org/10.1007/s00704-016-2031-3>, 2018.
- 895
- 896
- 897 Matsueda, M., Mizuta, R. and Kusunoki, S.: Future change in wintertime atmospheric blocking simulated using a 20-
898 km-mesh atmospheric global circulation model, *J. Geophys. Res.*, 114, D12114, doi: 10.1029/2009JD011919, 2009.
- 899
- 900 Mizielinski, M. S., Roberts, M. J., Vidale, P. L., Schiemann, R., Demory, M.-E., Strachan, J., Edwards, T., Stephens,
901 A., Lawrence, B. N., Pritchard, M., Chiu, P., Iwi, A., Churchill, J., del Cano Novales, C., Kettleborough, J., Roseblade,
902 W., Selwood, P., Foster, M., Glover, M., and Malcolm, A.: High-resolution global climate modelling: the UPSCALE
903 project, a large-simulation campaign, *Geosci. Model Dev.*, 7, 1629–1640, doi:10.5194/gmd-7-1629-2014, 2014.
- 904
- 905 O'Brien, T. A., Collins, W. D., Kashinath, K., Rübel, O., Byna, S., Gu, J., Krishnan, H. and Ullrich, P. A.: Resolution
906 dependence of precipitation statistical fidelity in hindcast simulations, *J. Adv. Model. Earth Syst.*, 8, 976–990, doi:
907 10.1002/2016MS000671, 2016.
- 908
- 909 O'Reilly, C. H., Minobe, S. and Kuwano-Yoshida, A.: The influence of the Gulf Stream on wintertime European
910 blocking, *Clim. Dynam.*, 47, 1545–1567, <https://doi.org/10.1007/s00382-015-2919-0>, 2016.
- 911
- 912 Prein, A. F. and Gobiet, A.: Impacts of uncertainties in European gridded precipitation observations on regional climate
913 analysis, *Int. J. Climatol.*, 37, 305–327, doi:10.1002/joc.4706, 2017.
- 914
- 915 Prein, A. F., Langhans, W., Fosser, G., Ferrone, A., Ban, N., Goergen, K., Keller, M., Tölle, M., Gutjahr, O., Feser,
916 F., Brisson,
917 E., Kollet, S., Schmidli, J., Van Lipzig, N. P. M., and Leung, R.: A review on regional convection- permitting climate
918 modeling: Demonstrations, prospects, and challenges, *Rev. Geophys.*, 53, 323–361. doi: 10.1002/2014RG000475,
919 2015.
- 920
- 921 Prein, A.F., Gobiet, A., Truhetz, H., Keuler, K., Goergen, K., Teichmann, C., Fox Maule, C., van Meijgaard, E., Déqué,
922 M., Nikulin, G., Vautard, R., Colette, A., Kjellström, E., and Jacob, D.: Precipitation in the EURO-CORDEX 0.11° and
923 0.44° simulations: high resolution, high benefits?, *Clim. Dynam.*, 46, 383–412, doi: 10.1007/s00382-015-2589-y, 2016.
- 924
- 925 Pryor, S. C., Nikulin, G., and Jones, C.: Influence of spatial resolution on regional climate model derived wind climates,
926 *J. Geophys. Res.*, 117, D03117, doi:10.1029/2011JD016822, 2012



927

928 Roberts, M. J., Vidale, P. L., Senior, C., Hewitt, H. T., Bates, C., Berthou, S., Chang, P., Christensen, H. M., Danilov,
929 S., Demory, M. E., Griffies, S. M., Haarsma, R., Jung, T., Martin, G., Minobe, S., Ringler, T., Satoh, M., Schiemann,
930 R., Scoccimarro, E., Stephens, G. and Wehner, M.F.: The benefits of global high-resolution for climate simulation:
931 process-understanding and the enabling of stakeholder decisions at the regional scale.. *B. Am. Meteorol. Soc.*, 99,
932 2341–2359 <https://doi.org/10.1175/BAMS-D-15-00320.1>, 2018.

933

934 Ruti, P. M., Somot, S., Giorgi, F., Dubois, C., Flaounas, E., Obermann, A., Dell'Aquila, A., Pisacane, G., Harzallah,
935 A., Lombardi, E., Ahrens, B., Akhtar, N., Alias, A., Arsouze, T., Aznar, R., Bastin, S., Bartholy, J., Béranger, K.,
936 Beuvier, J., Bouffies-Cloch e, S., Brauch, J., Cabos, W., Calmanti, S., Calvet, J., Carillo, A., Conte, D., Coppola, E.,
937 Djurdjevic, V., Drobinski, P., Elizalde-Arellano, A., Gaertner, M., Gal n, P., Gallardo, C., Gualdi, S., Goncalves, M.,
938 Jorba, O., Jord , G., L'Heveder, B., Lebeau-pin-Brossier, C., Li, L., Liguori, G., Lionello, P., Maci s, D., Nabat, P.,
939  nol, B., Raikovic, B., Ramage, K., Sevault, F., Sannino, G., Struglia, M. V., Sanna, A., Torma, C., and Vervatis, V.:
940 Med-CORDEX Initiative for Mediterranean Climate Studies. *B. Am. Meteorol. Soc.*, 97, 1187–1208,
941 <https://doi.org/10.1175/BAMS-D-14-00176.1>, 2016

942

943 Schiemann, R., Demory, M. E., Shaffrey, L. C., Strachan, J., Vidale, P. L., Mizielinski, M. S., Roberts, M. J., Matsueda,
944 M., Wehner, M. F. and Jung, T.: The resolution sensitivity of Northern Hemisphere blocking in four 25-km
945 atmospheric global circulation models, *J. Climate.*, 30, 337–358, <https://doi.org/10.1175/JCLI-D-16-0100.1>, 2017.

946

947 Schiemann, R., Vidale, P. L., Shaffrey, L. C., Johnson, S. J., Roberts, M. J., Demory, M.-E., Mizielinski, M. S., and
948 Strachan, J.: Mean and extreme precipitation over European river basins better simulated in a 25 km AGCM, *Hydrol.*
949 *Earth Syst. Sci.*, 22, 3933-3950, <https://doi.org/10.5194/hess-22-3933-2018>, 2018.

950

951 Seneviratne, S. I., Nicholls, N., Easterling, D., Goodess, C. M., Kanae, S., Kossin, J., Luo, Y., Marengo, J., McInnes,
952 K., Rahimi, M., Reichstein, M., Sorteberg, A., Vera, C. and Zhang, X.: Changes in climate extremes and their impacts
953 on the natural physical environment. In: *Managing the Risks of Extreme Events and Disasters to Advance Climate*
954 *Change Adaptation. A Special Report of Working Groups I and II of the Intergovernmental Panel on Climate Change*,
955 edited by: Field, C. B., Barros, V., Stocker, T. F., Qin, D., Dokken, D. J., Ebi, K., L. Mastrandrea, M. D., Mach, K.
956 J., Plattner, G.-K., Allen, S. K., Tignor, M. and Midgley, P. M., Cambridge University Press, Cambridge, UK, and
957 New York, NY, USA, pp. 109-230, 2012

958

959 Shields, C. A., Kiehl, J. T., and Meehl, G. A.: Future changes in regional precipitation simulated by a half-degree
960 coupled climate model: Sensitivity to horizontal resolution, *J. Adv. Model. Earth Syst.*, 8, 863–884, doi:
961 10.1002/2015MS000584, 2016.

962



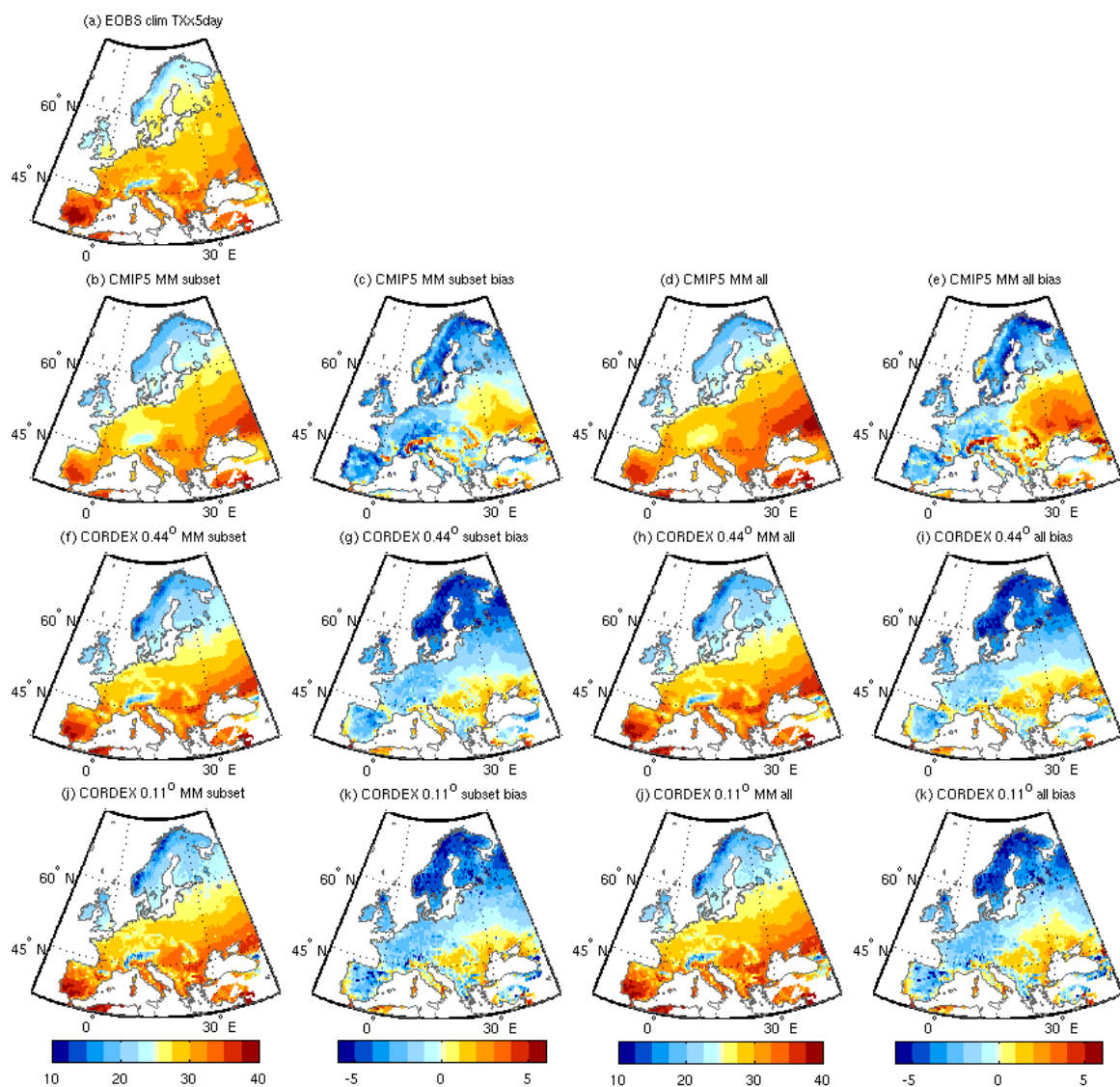
- 963 Stott, P. A., Christidis, N., Otto, F. E., Sun, Y., Vanderlinden, J., van Oldenborgh, G. J., Vautard, R., von Storch, H.,
964 Walton, P., Yiou, P. and Zwiers, F. W.: Attribution of extreme weather and climate- related events. *WIREs Clim.*
965 *Change*, 7, 23-41. doi:10.1002/wcc.380, 2016.
- 966
- 967 Taylor, K., Williamson, D., and Zwiers, F.: The sea surface temperature and sea-ice concentration boundary conditions
968 for AMIP II simulations, PCMDI Rep. 60, Tech. Rep. 60, PCMDI, 25 pp., available at: [http://www-](http://www-pcmdi.llnl.gov/publications/ab60.html)
969 [pcmdi.llnl.gov/publications/ab60.html](http://www-pcmdi.llnl.gov/publications/ab60.html), 2000.
- 970
- 971 Taylor, K. E., Stouffer, R. J. and Meehl, G. A.: An overview of CMIP5 and the experiment design, *B. Am. Meteorol.*
972 *Soc.*, 93, 485498, doi: 10.1175/BAMS-D-11-00094.1, 2012.
- 973
- 974 Terai, C. R., Caldwell, P. M., Klein, S. A. Tang, Q. and Branstetter, M. L.: The atmospheric hydrologic cycle in the
975 ACME v0.3 model. *Clim. Dynam.*, 50, 3251- 3279. <https://doi.org/10.1007/s00382-017-3803-x>, 2018.
- 976
- 977 Torma, C., Giorgi, F. and Coppola, E.: Added value of regional climate modeling over areas characterized by complex
978 terrain—Precipitation over the Alps, *J. Geophys. Res. Atmos.*, 120, 3957–3972, doi: 10.1002/2014JD022781, 2015.
- 979
- 980 Van Haren, R., Haarsma, R. J., Van Oldenborgh, G. J. and Hazeleger, W.: Resolution Dependence of European
981 Precipitation in a State-of-the-Art Atmospheric General Circulation Model, *J. Climate.*, 28, 5134–5149, doi:
982 10.1175/JCLI-D-14-00279.1, 2015a.
- 983
- 984 Van Haren, R., Haarsma, R. J., de Vries, H., van Oldenborgh, G. J., and Hazeleger, W.: Resolution dependence of
985 circulation forced future central European summer drying, *Environ. Res. Lett.*, 10, 055002, doi:10.1088/1748-
986 9326/10/5/055002, 2015b.
- 987
- 988 Vanniere, B., Vidale, P. L., Demory, M.-E., Schiemann, R., Roberts, M. J., Roberts, C. D., Matsueda, M., Terray, L.,
989 Koenigk, T., Senan, R.: Multi-model evaluation of the sensitivity of the global energy budget and hydrological cycle
990 to resolution, *Clim. Dynam.*, 52, 6817- 6846, <https://doi.org/10.1007/s00382-018-4547-y>, 2019
- 991
- 992 Vautard, R., Gobiet, A., Jacob, D., Belda, M., Colette, A., Déqué, M., Fernández, J., García-Díez, M., Goergen, K.,
993 Güttler, I., Halenka, T., Karacostas, T., Katragkou, E., Keuler, K., Kotlarski, S., Mayer, S., van Meijgaard, E., Nikulin,
994 G., Patarcic, M., Scinocca, J., Sobolowski, S., Suklitsch, M., Teichmann, C., Warrach-Sagi, K., Wulfmeyer, V., Yiou,
995 P. : The simulation of European heat waves from an ensemble of regional climate models within the EURO-CORDEX
996 project, *Clim. Dynam.*, 41, 2555-2575, doi: 10.1007/s00382-013-1714-z, 2013.
- 997
- 998 Vautard, R., Yiou, P., Otto, F., Stott, P., Christidis, N., van Oldenborgh, G. J. and Schaller, N.: Attribution of human-
999 induced dynamical and thermodynamical contributions in extreme weather events, *Environ. Res. Lett.*, 11, 114009,
1000 <https://doi.org/10.1088/1748-9326/11/11/114009>, 2016.



1001
1002
1003 Volosciuk, C., Maraun, D., Semenov, V.A. and Park, W.: Extreme Precipitation in an Atmosphere General Circulation
1004 Model: Impact of Horizontal and Vertical Model Resolutions, *J. Climate.*, 28, 1184–1205,
1005 <https://doi.org/10.1175/JCLI-D-14-00337.1>, 2015.
1006
1007 Vries, H. de, Scher, S., Haarsma, R., Drijfhout, S., and Delden, A. van.: How Gulf-Stream SST-fronts influence
1008 Atlantic winter storms, *Clim. Dynam.*, 52, 5899-5909. <https://doi.org/10.1007/s00382-018-4486-7>, 2019
1009
1010 Weedon, G. P., Balsamo, G., Bellouin, N., Gomes, S., Best, M. J. and Viterbo, P., The WFDEI meteorological forcing
1011 data set: WATCH Forcing Data methodology applied to ERA-Interim reanalysis data, *Water Resour. Res.*, 50, 7505–
1012 7514, doi:10.1002/2014WR015638, 2014.
1013
1014 Wehner, M. F., Smith, R. L., Bala, G. and Duffy, P.: The effect of horizontal resolution on simulation of very extreme
1015 US precipitation events in a global atmosphere model, *Clim. Dynam.*, 34, 241-247. [https://doi.org/10.1007/s00382-](https://doi.org/10.1007/s00382-009-0656-y)
1016 [009-0656-y](https://doi.org/10.1007/s00382-009-0656-y), 2010.
1017
1018 Wehner, M. F., Reed, K. A., Li, F., Prabhat, Bacmeister, J., Chen, C.- T., Paciorek, C., Gleckler, P. J., Sperber, K. R.,
1019 Collins, W. D., Gettelman, A., and Jablonowski, C.: The effect of horizontal resolution on simulation quality in the
1020 Community Atmospheric Model, CAM5.1, *J. Adv. Model. Earth Syst.*, 6, 980–997, doi:10.1002/2013MS000276,
1021 2014.
1022
1023 Willison, J., Robinson, W.A. and Lackmann, G.M.: North Atlantic Storm-Track Sensitivity to Warming Increases with
1024 Model Resolution, *J. Climate.*, 28, 4513–4524, <https://doi.org/10.1175/JCLI-D-14-00715.1>, 2015.
1025
1026 Zappa, G., Shaffrey, L. C. and Hodges, K. I., The Ability of CMIP5 Models to Simulate North Atlantic Extratropical
1027 Cyclones, *J. Climate.*, 26, 5379-5396, doi: 10.1175/JCLI-D-12-00501.1, 2013.
1028
1029 Zhang, X., Alexander, L., Hegerl, G. C., Jones, P., Tank, A. K., Peterson, T. C. Trewin, B. and Zwiers, F. W.: Indices
1030 for monitoring changes in extremes based on daily temperature and precipitation data, *Wiley Interdiscip. Rev., Clim.*
1031 *Chang.*, 2, 851–870, doi:10.1002/wcc.147, 2011.
1032
1033
1034



1035 **Figures**

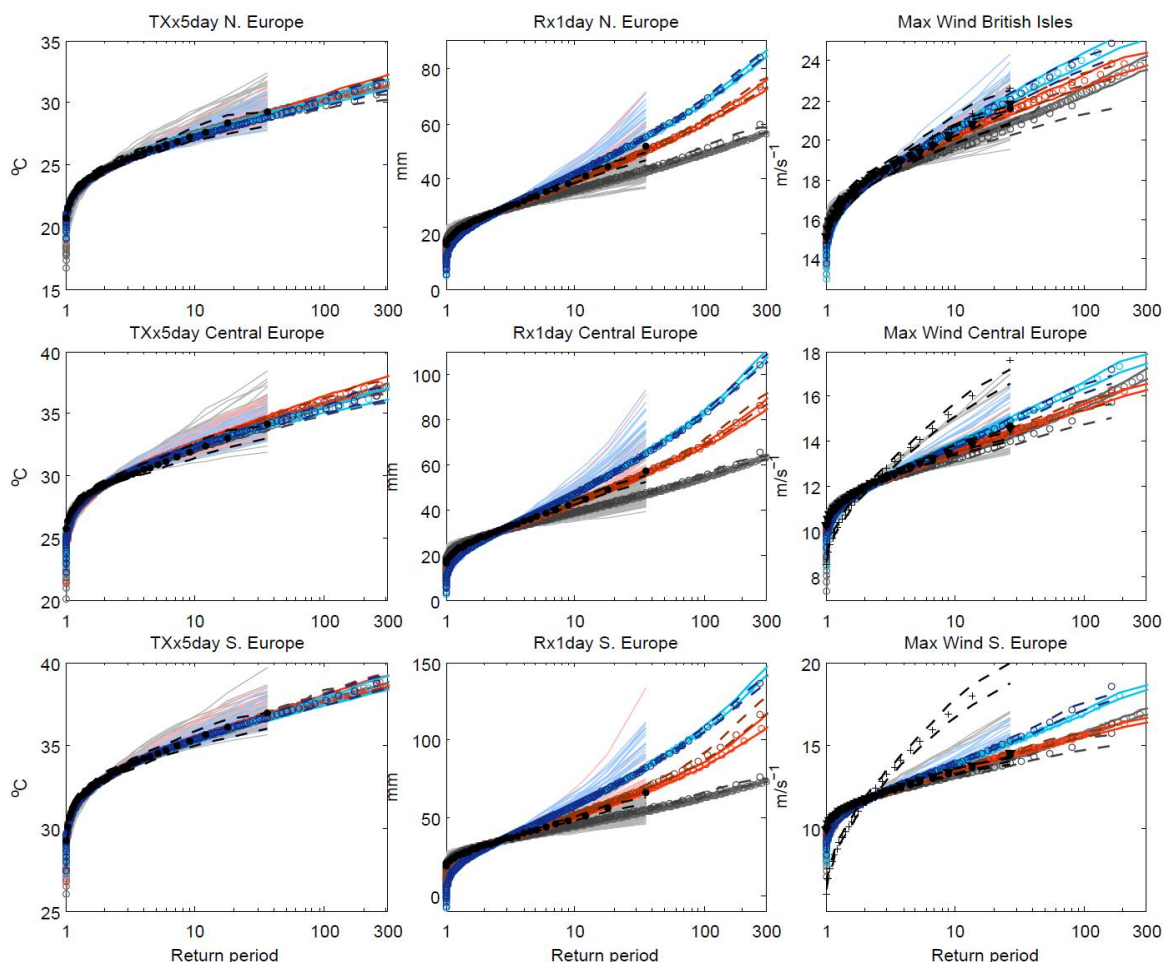


1036

1037 **Figure 1:** Climatological mean of TXx5day for the period 1970-2005 for (a) EOBS, the multi model mean of the common
1038 subset of models for (b) CMIP5, (f) CORDEX 0.44° and (j) CORDEX 0.11°, (c, g, k) their biases with respect to EOBS, and
1039 (d,e,h,i,j,k) the same for the full ensembles of CMIP5, and CORDEX. Units °C.

1040

1041



1042



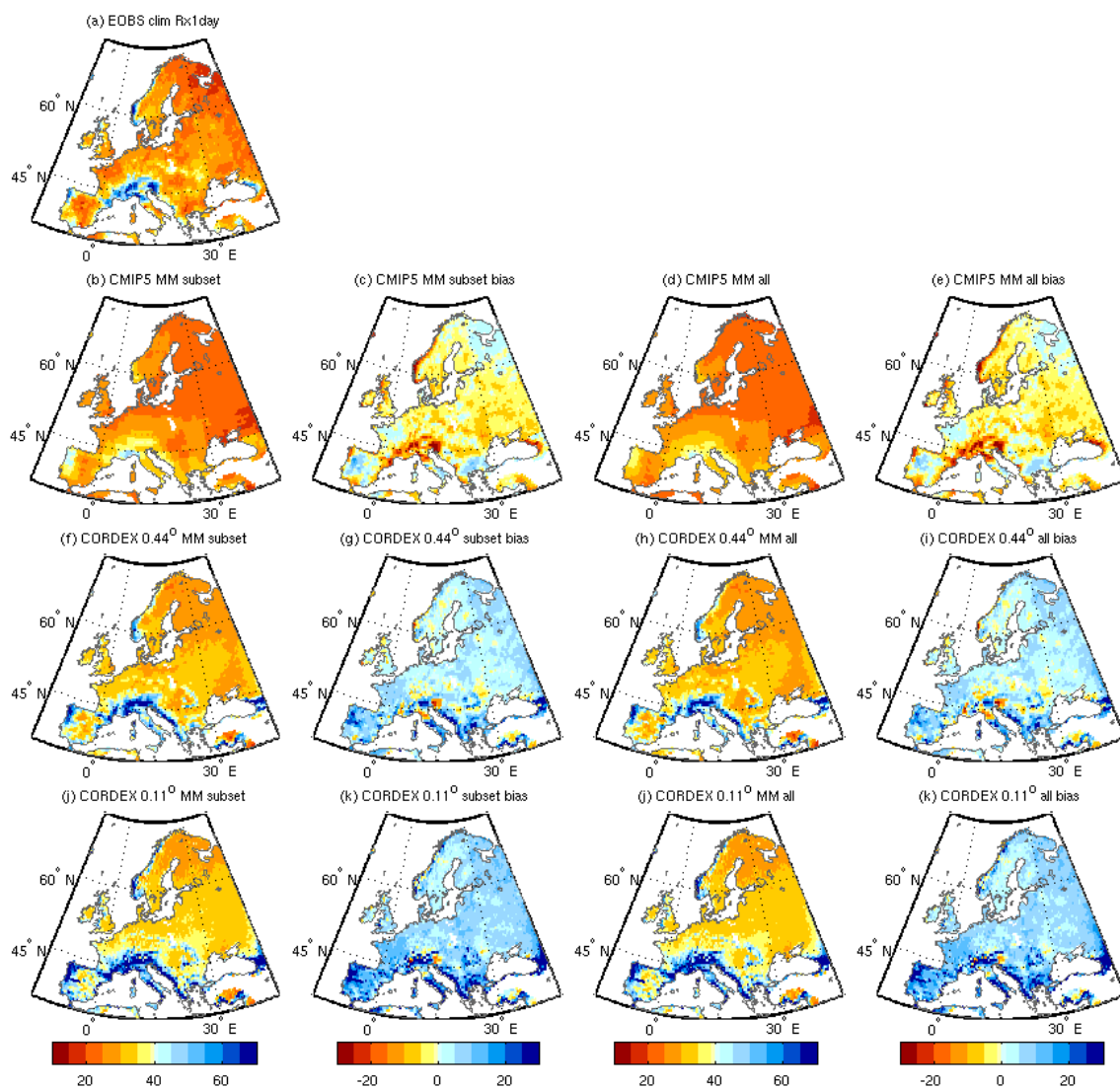
1043

1044

1045 **Figure 2: Return period plots for (left) TXx5day, middle column Rx1day and (right) annual maximum wind, for CMIP5**
 1046 **and CORDEX for Northern Europe (top row except top left = British Isles), Central Europe (middle row) and Southern**
 1047 **Europe (bottom row). CMIP5 is shown in grey, CORDEX 0.44° in red and CORDEX 0.11° in blue. Thin lines are individual**
 1048 **ensemble members, circles represent the pooled ensembles, lighter shades for the full ensembles, and darker shades for the**
 1049 **subset of models common to CMIP5, and both CORDEX resolutions. Observations are shown in black, circles for E-OBS**
 1050 **temperature and precipitation and WFDEI wind, triangles for MESAN precipitation and ECEM noc wind and crosses for**
 1051 **ECEM wbc wind. Confidence intervals based on bootstrapping are shown with dashed lines. The time periods considered**
 1052 **are 1970-2005 for TXx5day and Rx1day, and 1979-2005 for wind.**

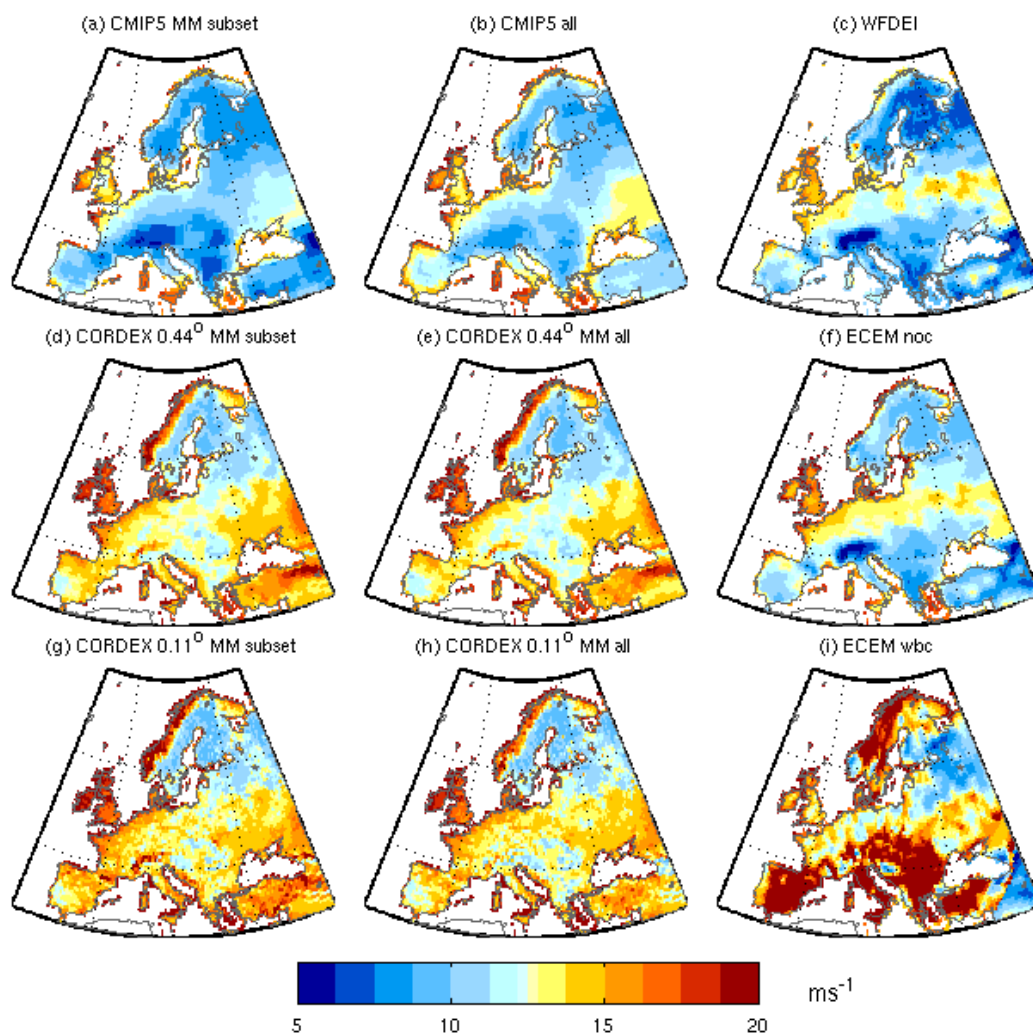
1053

1054



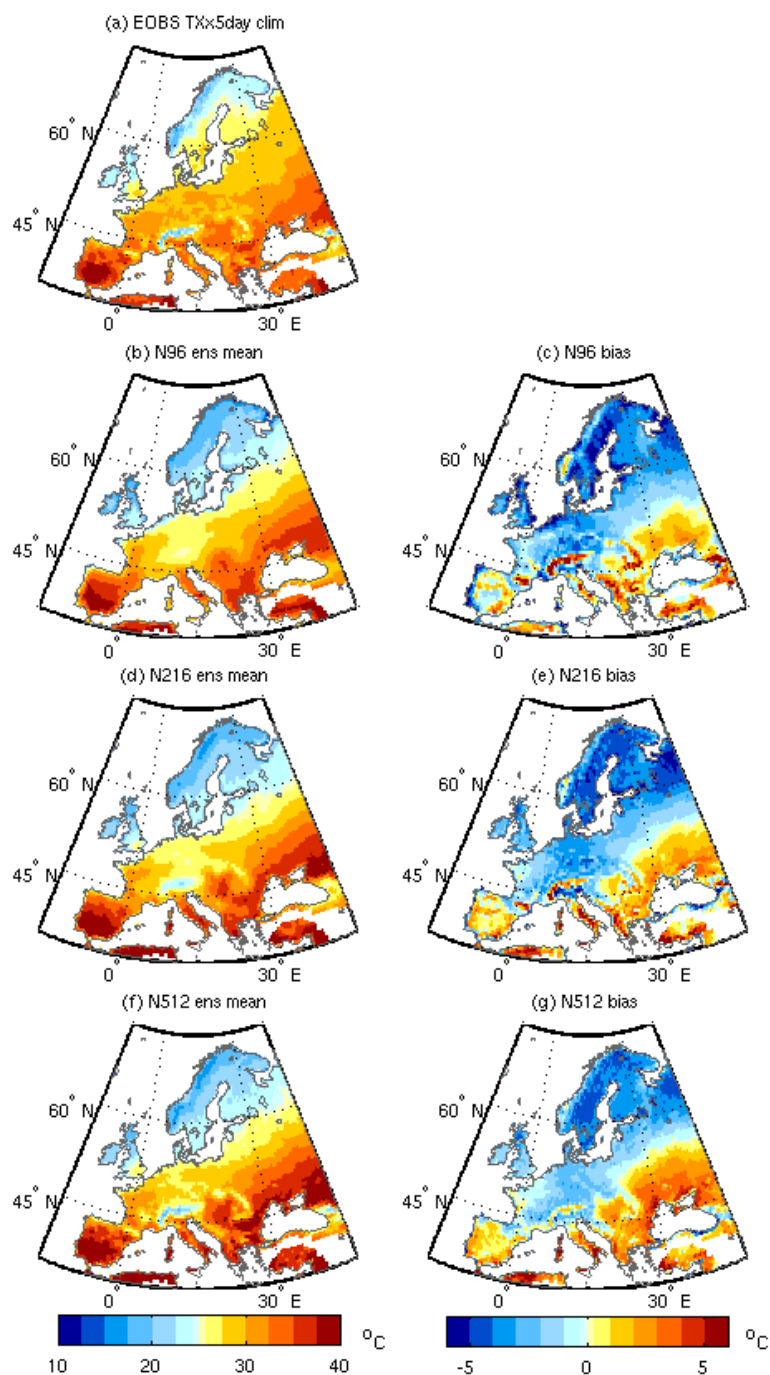
1055

1056 **Figure 3: As for Figure 1 but for the climatological mean of Rx1day. Units mm.**

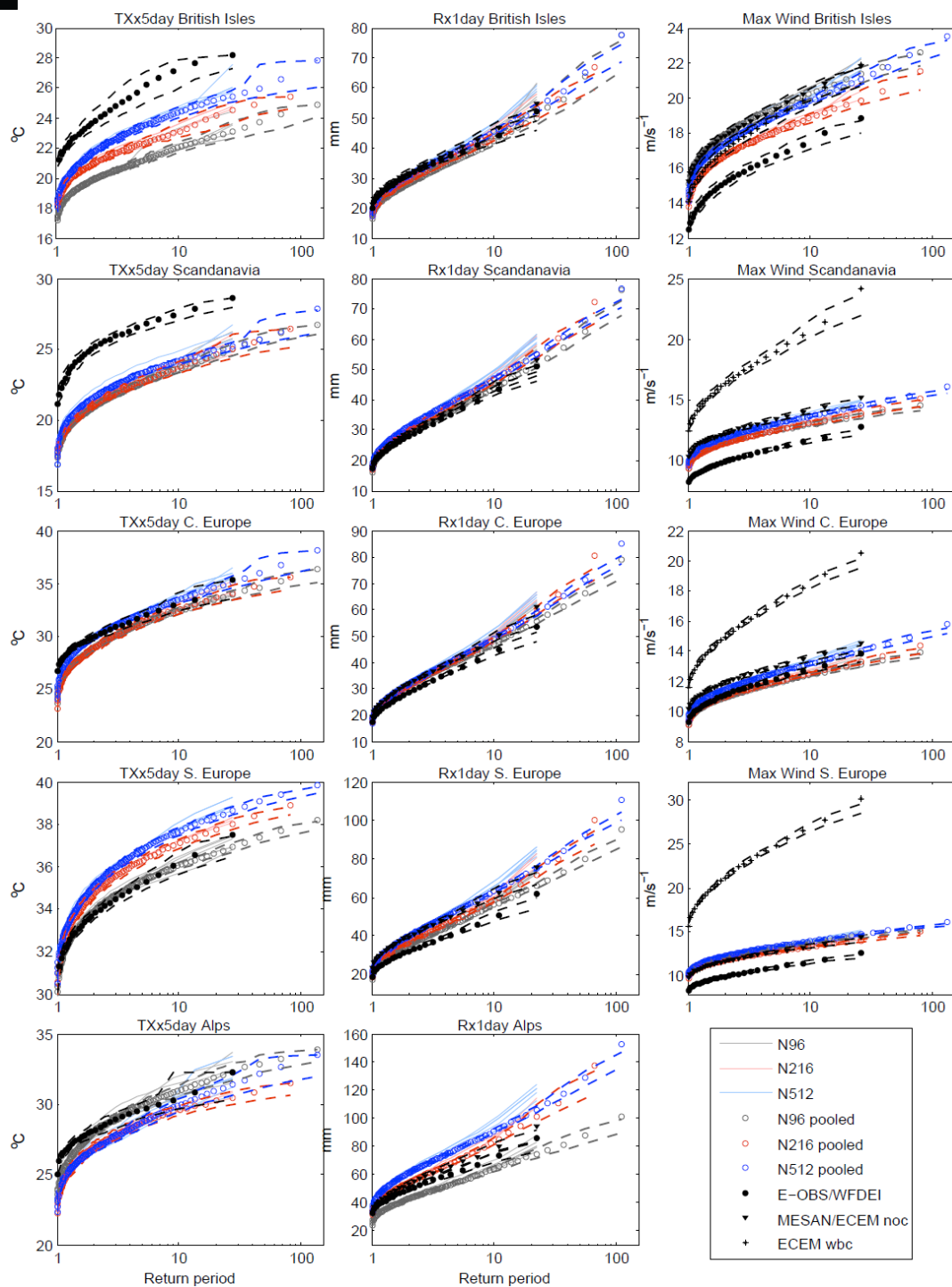


1057
1058

1059 **Figure 4:** Climatological mean of annual maximum of daily maximum wind for the period 1979-2005 for the multi model
1060 mean of the common subset of models for (a) CMIP5, (d) CORDEX 0.44° and (g) CORDEX 0.11°, (b, e, h) the same for the
1061 full ensembles of CMIP5 and CORDEX, and the observational datasets (c) WFDEI, (f) ECEM noc (i) ECEM wbc. Units
1062 meters per second.



1065 **Figure 5:** Climatological mean of TXx5day for the ensemble means of three resolutions of HadGEM3-A (UPSCALE) GCM simulations (left) for the period 1985-2011 and their biases with respect to E-OBS (right). (a) EOBS, (b, c) N96 (130 km), (d, e) N216 (60 km), (f, g) N512 (25 km). Units °C.



1070 **Figure 6: Return period plots for (left) TXx5day, middle column Rx1day and (right) annual maximum wind, for the UPSCALE simulations for (top row) the British Isles, (2nd row) Scandinavia, (3rd row) Central Europe, (4th row) Southern Europe, and (last row) the Alps. N96 is shown in grey, N216 in red and N512 in blue. Thin lines are individual ensemble members, circles represent**



the pooled ensembles. Observations are shown in black, circles for E-OBS and WFDEI, triangles for MESAN and ECEM noc, and asterisks for ECEM wbc. Confidence intervals based on bootstrapping are shown with dashed lines. The time periods considered are 1985-2011 for TXx5day, 1989-2010 for Rx1day, and 1986-2011 for wind. NB: there is no bias correction of the climatology (see methods).

1075

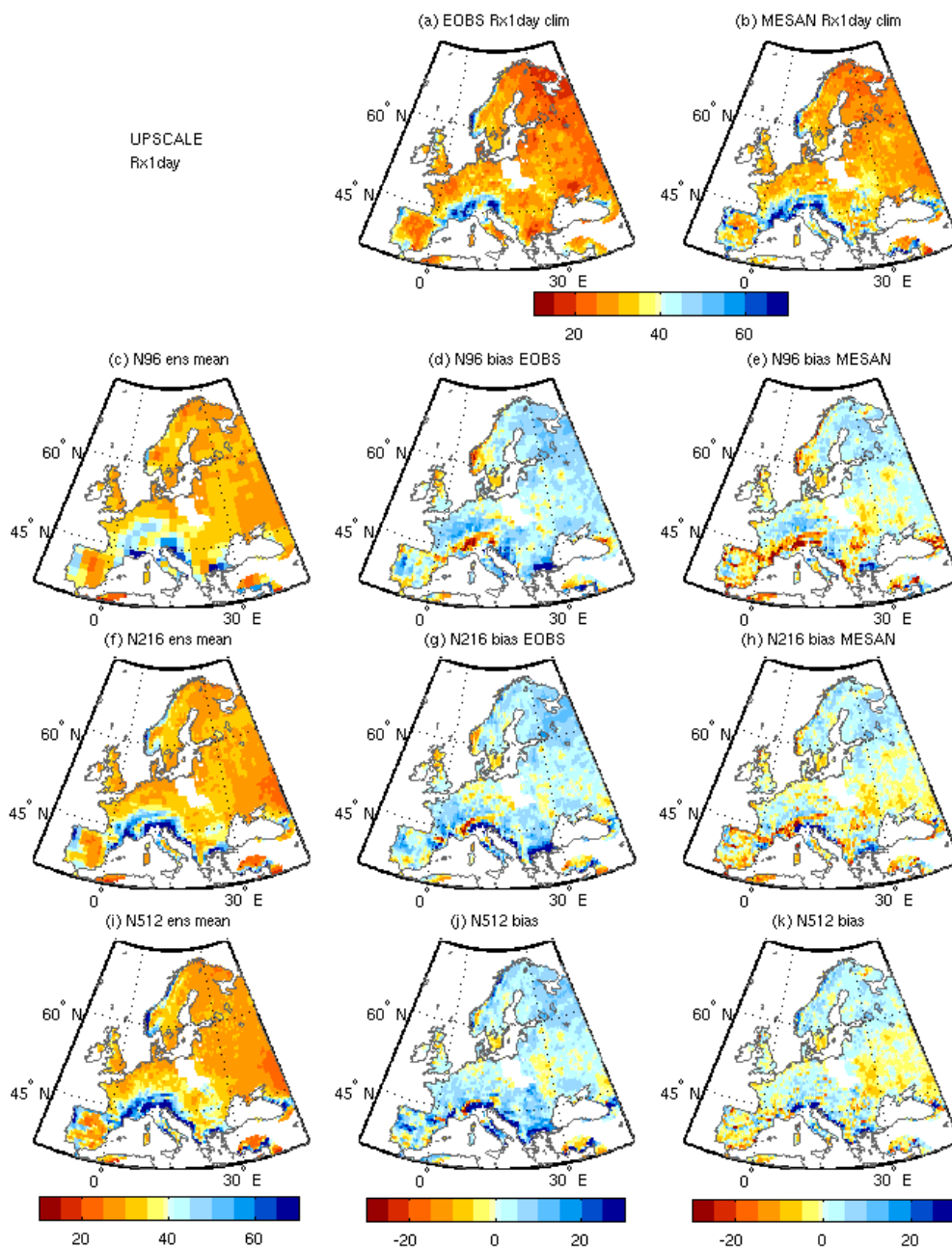
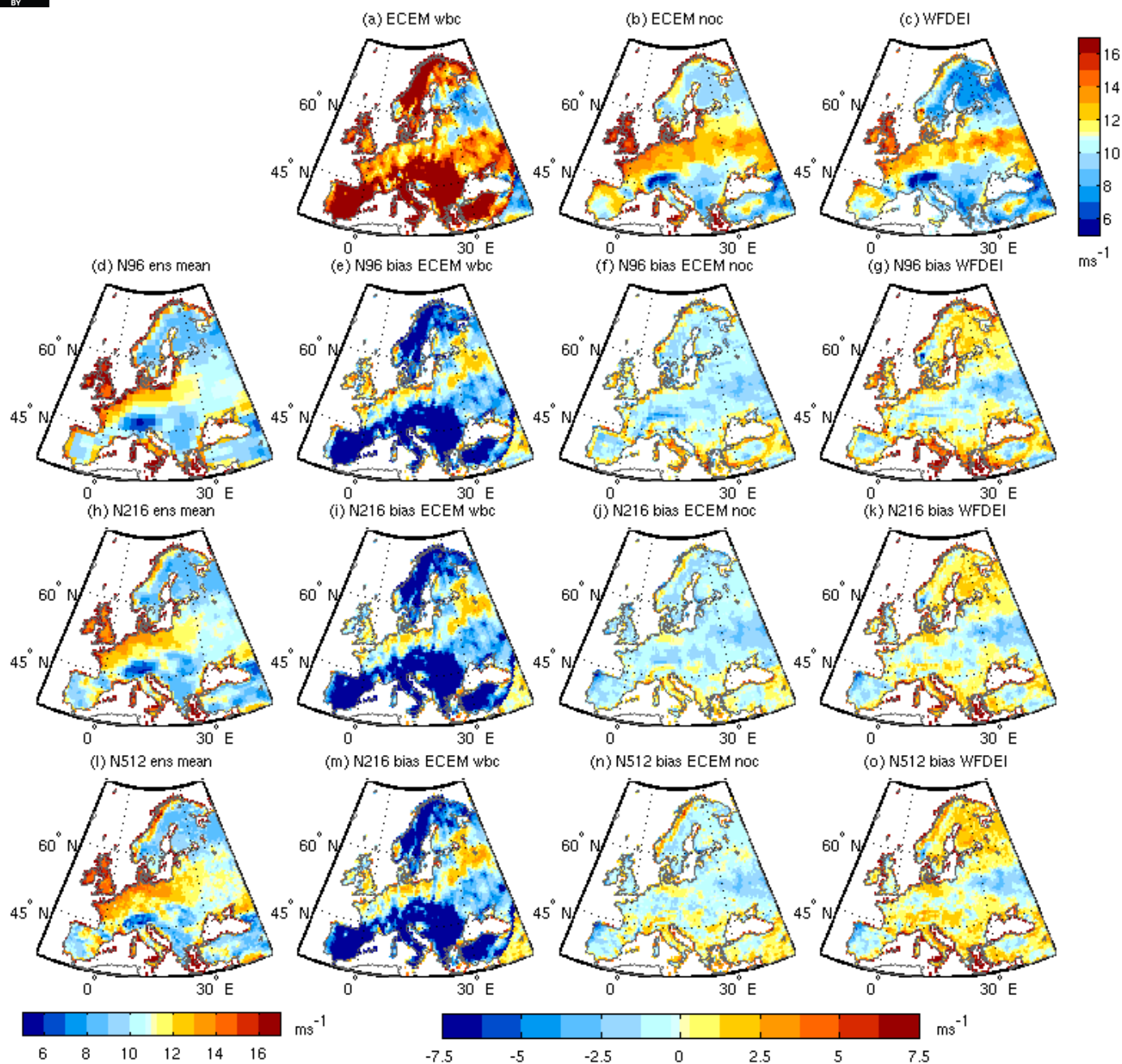
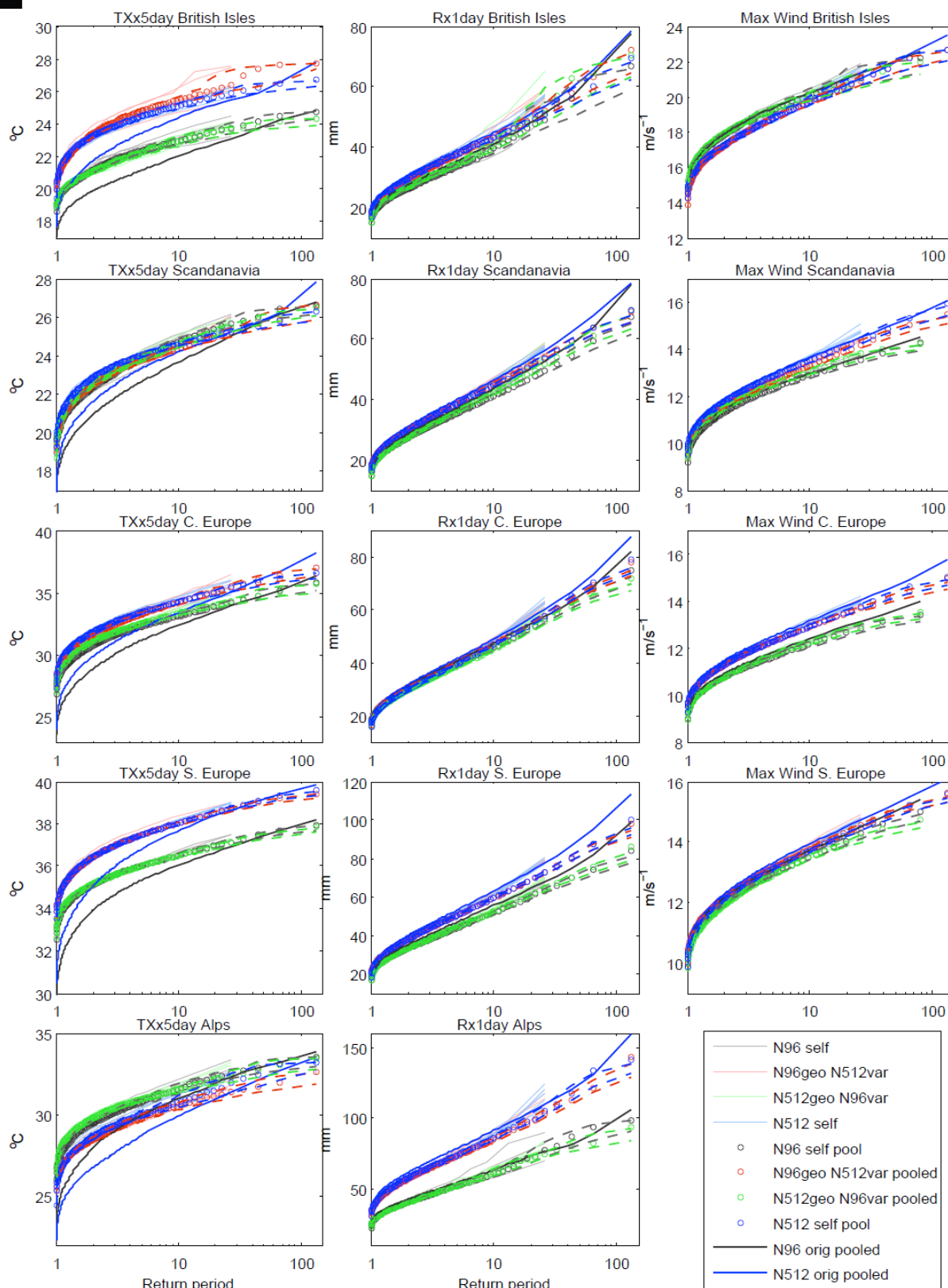


Figure 7: Climatological mean of Rx1day for the ensemble means of three resolutions of UPSCALE (left) simulations for the period 1989-2010 and their biases with respect to E-OBS (middle) and the MESAN reanalysis (right). (a) EOBS, (b) MESAN (c-e) N96, (f-h) N216, (i-k) N512. Units mm.



1080 **Figure 8:** Climatological mean of annual maximum wind for the ensemble means of three resolutions of UPSCALE (left) simulations for the period 1986-2011 and their biases with respect to the observational datasets ECEM wbc (left), ECEM noc (middle) and WFDEI (right). (a) ECEM wbc, (b) ECEM noc (c) WFDEI, (d-g) N96, (h-k) N216, (l-o) N512. Units meters per second.





1085 **Figure 9: Circulation analogue results. Return period plots for (left) TXx5day, (middle) Rx1day and (right) annual maximum wind**
for (top) the British Isles, (2nd row) Scandinavia, (3rd row) Central Europe, (4th row) Southern Europe and (5th row) the Alps. Grey
represents the N96 self-analogues, blue the N512 self-analogues, red is for N96 circulation with N512 variables (e.g. precipitation)
and green is for N512 circulation with N96 variables. Thin lines represent individual ensemble members, circles represent results
pooled across ensemble members. Dashed lines are 5-95% confidence intervals based on a bootstrapping technique. Thick blue line
1090 represents the original pooled N512 results like those shown in Figure 6 (although sometimes based on a different time period), and
the thick grey line represents the equivalent for the N96 simulations. Results for TXx5day are based on the period 1985-2011, Rx1day
1986-2011, and wind 1986-2011.